ON THE DESIGN, CONSTRUCTION, CALIBRATION, AND TESTING OF A CUSTOM LANGMUIR PROBE FOR USE IN AN RF PLASMA CHAMBER

by

Andres Edelmiro De La Garza, B.S.

A thesis submitted to the Graduate Council of
Texas State University in partial fulfillment
of the requirements for the degree of
Master of Science
with a Major in Physics
December 2019

Committee Members:

Edwin L. Piner, Chair

Wilhelmus J. Geerts

Karl D. Stephan

FAIR USE AND AUTHOR'S PERMISSION STATEMENT

Fair Use

Duplication Permission

ACKNOWLEDGMENTS

I would like to first and foremost give thanks to Dr. Karl D. Stephan who has invested his time and energy on both my development as a young scientist as well as to his current experimental setup which he has allowed me to lend a helping hand in. Working for Dr. Stephan has really brought to my attention how much I enjoy the process of designing, building, testing, and iterating solutions to problems that arise in the context of an experimental physics laboratory. Without Dr. Stephan's unmatched persistence to complete his goals and expert guidance with regards to electronics for scientific measurements and plasma science I can say with certainty that I would not have found a path within the sciences that I full-heartedly would like to continue on. I thank Dr. Stephan for becoming an inspiration to me and a standard by which I can compare how well I too am working towards achieving my goals. Lastly, I would like to thank him for showing me all that can be accomplished when you are disciplined and stay dedicated to what truly matters to you regardless of what is going on around you. I would also like to thank Yue Hua our visiting scholar and friend from Dilan, China for construction of the Langmuir probes and being a good friend.

I would also like to thank my parents, Mario and Elisa De La Garza as well as my two brothers Mario Jr. and Eduardo De La Garza for all of their support and unconditional love they have given me even when I am not the nicest person to be around. I know that they will support me though all my endeavors regardless of how unconventional they may become.

TABLE OF CONTENTS

Page

LIST OF TABLES

Table **Page**

LIST OF FIGURES

Figure **Page**

ABSTRACT

A particular interest of the principal investigator regarding a rare atmospheric phenomenon called ball lightning influenced the design and construction of a custom RF plasma chamber. However, the primary focus of this experiment is not on the ball lightning but instead on the interesting phenomenon that occurs when RF plasma is near its plasma frequency. At its plasma frequency, it behaves as a metamaterial which are said to exhibit interesting microwave properties. A Langmuir probe was needed to be built to collect data on the plasma density and find relationships between plasma density and how well it acts as a waveguide.

A custom plasma chamber was then designed and built for the purpose of testing the microwave attenuation/dispersion characteristics (S-parameters) of a cylindrically symmetric RF plasma (13.56 MHz). The principal investigator was interested in studying how plasma electron density affects waveguide dispersion characteristics.

Since commercially available Langmuir probes were beyond the project budget a Langmuir probe as well as the associated sensing circuitry was designed, built, tested and calibrated in-house. The necessary theoretical background needed to understand the probe and sensing circuitry is presented as well as construction of the probe and sense circuitry.

I. INTRODUCTION

The purpose of this work is to give enough background information on Langmuir probe theory as well as a detailed guide on the steps taken to build, test and calibrate a Langmuir probe for the purpose of determining electrical parameters of interest from an inductively coupled RF plasma. The principal investigator of this master's thesis project has a unique interest in a rare atmospheric phenomenon called "Ball Lightning". Recently, he came across a publication by Wu called "Relativistic-microwave theory of ball lightning" where Wu proposes a theory to the mechanism by which ball lightning is formed. [1] As described by Wu [1], ball lightning is an unexplained fireball-like object that tends to occur during thunderstorms. In Wu's publication "Relativistic-microwave theory of ball lightning" he explains how before lightning strikes the ground, electrons at the end of the lightning bolt can reach relativistic speeds which emit intense microwave radiation. The intense radiation is said to ionize the surrounding air as well as evacuate a plasma bubble that effectively contains the microwave radiation in a stable spherical configuration for a short duration of time.

Although the principal investigator's main goal is to discover the mechanism by which ball lightning works in nature, funding for this type of study was simply out of reach at the time of this writing. However, funding for investigating metamaterials, which have gained popularity among certain scientific circles recently, was available. So, a study that contained aspects of Wu's theory as well as investigating the nature of metamaterials was designed.

To give more detail on metamaterials, they are materials that have properties not typically found in nature, and more specifically those with epsilon-near-zero (ENZ) characteristics, meaning their dielectric constants are near zero, have shown to exhibit interesting properties. Of the mentioned metamaterials, RF plasma near the plasma frequency has shown to exhibit ENZ behavior. This fact, along with the principle investigator's interest in ball lighting inspired an experiment that would test attenuation/dispersion characteristics of microwave-plasma interactions.

The experiment involves using a microwave analyzer (Keysight N9917A network analyzer) to transmit and measure the intensity of microwave radiation transmitted through an air space surrounded by a plasma with cylindrical symmetry acting as a waveguide. In this experiment, the intensity of microwave scattering (S-parameters) are dependent on the density of the plasma which is typically gauged by how many free electrons occupy a unit volume. This plasma parameter is also known as the electron density, given by n_e. The parameters n_e along with other plasma parameters can be derived from plasma I-V data collected using a Langmuir probe. Methods used to measure these plasma parameters are without a doubt commercially available; however, these tools are relatively expensive and not necessarily designed to fit in the custom built RF plasma system. Of the methods of characterizing plasma parameters a simple Langmuir probe is by far the easiest solution to manufacture. With that being said the task to design, build, test, and calibrate a Langmuir probe for determination of electron density first and of second importance the electron temperature (T_e) was assigned as the goal of this master's thesis.

As mentioned above, a simple Langmuir probe is the easiest method to implement for n_e and T_e determination. However, those attempting to make a probe still will be faced with some challenges. For example, performing the measurements mentioned above in an RF plasma environment without the proper compensation circuitry can cause erroneous data collection and as a result invalid plasma parameter determination. The method used in this study to negate the negative effects of fluctuating RF plasma potentials is through the use of passive RF compensation circuitry.

Passive RF compensation circuitry in this sense, means to add chokes (inductors) whose resonant frequencies are tuned to the RF plasma frequency and its second harmonic. The chokes are placed as close to the probe tip as possible and form a high impedance path to the RF looking in from the plasma to the sensing portion of the probe, and a low impedance path to low frequency sweep signals (essentially DC signals) looking from the sensing circuitry into the plasma. A high impedance to the RF oscillations to the sensing circuitry attenuates the RF voltage swings and ideally would eliminate the swing altogether allowing for a perfect measurement to be made. However, reasonable RF compensation, considering probe dimensions and the particular RF plasma chamber in this work, will not completely eliminate all of the RF oscillations but will attenuate the unwanted signals to a degree that allows for reasonably accurate data to be collected and in turn good approximations of the plasma parameters to be determined.

Summarizing what has been stated thus far, a discussion in what follows will be given over: 1) necessary probe theory will be discussed in sufficient detail to help the reader understand why the probe and associated circuitry was built the way it was, 2) detailed procedures are given to tell how the probe was constructed, 3) detailed procedure

will be given explaining how the sensing circuitry for this Langmuir probe was designed, built, and calibrated, 4) a section on data analysis and numerical methods used to calculate the plasma parameters of interest.

II. PROBE THEORY

A Langmuir probe is used to measure charged particle flux from a plasma source. In doing so one can obtain an I-V plasma characteristic curve from which plasma parameters can be deduced. The probe is inserted into the plasma and the electric potential of the probe is changed with respect to the plasma floating potential. Due to the electric gradient between the plasma and probe, a net particle flux arises. Net particle flux, electric current, is measured and the corresponding voltage of the probe is recorded. This process is repeated for a range of probe bias voltages and as a result, the I-V plasma characteristic is obtained.

As simple as the above measurement may sound, the experimentalist is quickly faced with questioning the perturbing effects of the probe on the plasma. Consideration must be given to how a local change of the electric field at the probe affects the plasma far away from the probe. The goal then, is to obtain a plasma characteristic curve from the locally perturbed region of the plasma and somehow relate the characteristic back to the unperturbed plasma environment. Introduction of a Langmuir probe inherently causes the plasma's electrical characteristics to change locally and the goal is to find a way to relate the current and voltage measured in the vicinity of the probe to the characteristics of the plasma far away from the perturbing source where we assume perturbing affects are negligible.

The reason why introduction of a Langmuir probe causes a perturbation of the plasma can be explained by considering elementary gas-kinetic theory. The theory tells us that for a given species of gas particles crossing a unit area per unit time the particle flux is given by (2.1). [2]

$$\Gamma = \frac{1}{4} n \bar{v} \tag{2.1}$$

In (2.1) above, Γ, n, and $\bar{v}$ are the net particle flux, particle density number, and average particle speed in one direction respectively. From kinetic gas theory, we know that when comparing particle speeds of different masses but with similar energy the more massive particles move slower than do their less massive counterparts.

Now, imagining that initially, we insert a charge neutral probe into the plasma environment, as time progresses the probe becomes negatively charged. This happens because, on average, the faster moving particles tend to collide into the probe at a higher frequency than do the slower moving heavier positively charged particles. So, for a probe of total surface area A we get a total electric current given by (2.2). Equation (2.2) tells us that a positive current moves into the probe if we assume the electron average speed ($\bar{v}_e$) is much greater than the ion average speed ($\bar{v}_i$). [2]

$$I = -eA\left(\frac{1}{4} n_i \bar{v}_i - \frac{1}{4} n_e \bar{v}_e\right) \approx \frac{1}{4} e A n_e \bar{v}_e \tag{2.2}$$

If however, for the moment we assume that the probe is not connected to any external circuitry and the probe is isolated from a solid connection to ground, what happens is that the probe builds up a net negative charge effectively perturbing the plasma potential in the vicinity of the probe. The accumulation of negative charges on the probe will cause positive space charge to build around it and if one considers a simplified version of Poisson's equation for the situation at hand the solution to Poisson's equation gives that the perturbing effects of the probe will only reach a few Debye length into the plasma. [2] This is due to the exponential dependence of the potential as a function of the

distance away from the probe on the scale of the characteristic Debye length. The electron Debye length is given by (2.3) where T_e, and n_∞ are the electron temperature and particle number density far away from the perturbing source.

$$\lambda_D = \sqrt{\frac{\epsilon_0 T_e}{e^2 n_\infty}} \tag{2.3}$$

The phenomenon described in the last paragraph is called Debye shielding and is the reason why the perturbing effects of objects inserted into a plasma environment do not affect the bulk of the plasma. The region from the probe to where the plasma reaches quasineutrality is called a space charge sheath, or more compactly, the sheath. [3] The sheath is predominantly positively charged ions.

The plasma sheath that forms around a Langmuir probe is typically on the order or a few Debye lengths thick. The edge of the sheath, in the direction away from the probe, is where the plasma is defined to establish quasineutrality, meaning that the number of ions and electrons is roughly the same. On the other hand, as we approach the probe, there is a decrease in the number of free electrons due to more collision on average of electrons with the probe than ions. As a result, there is an excess ion concentration responsible for the shielding effects to the plasma discussed above.

Below is a schematic diagram of the sheath formation. In the Figure 1 below the probe edge is located at $x = 0$ and the region of charge imbalance is found in the region $-d < x < 0$, the sheath region. $x = -d$ is the distance from the probe required for the plasma to approximately establish charge neutrality. Between $-\lambda_{\text{mfp}} < x < -d$ the ion and electron number densities are roughly equal, and the region serves as the space

connecting the conditions found in the sheath to those of the unperturbed plasma. This region is called the transition region or the presheath and roughly spans one ion mean free path (λ_{mfp}). Passed the presheath is the unperturbed plasma region or the bulk plasma.

Without a derivation, the Child-Langmuir law (2.3) is a mathematical relationship between the potential drop across the space charge sheath (U), the ion current density (j_i), and the thickness of the space charge sheath (d).

$$j_i = \frac{4}{9}\epsilon_0 \left(\frac{2e}{m_i}\right)^{\frac{1}{2}} \left(\frac{U^{\frac{3}{2}}}{d^2}\right) \tag{2.4}$$

It is said that for the plasma sheath U, is constant and the ion current is set by the conditions of the unperturbed plasma. [3] This means that the sheath thickness must change to accommodate changes in ion current densities to the probe. Although (2.3) is a

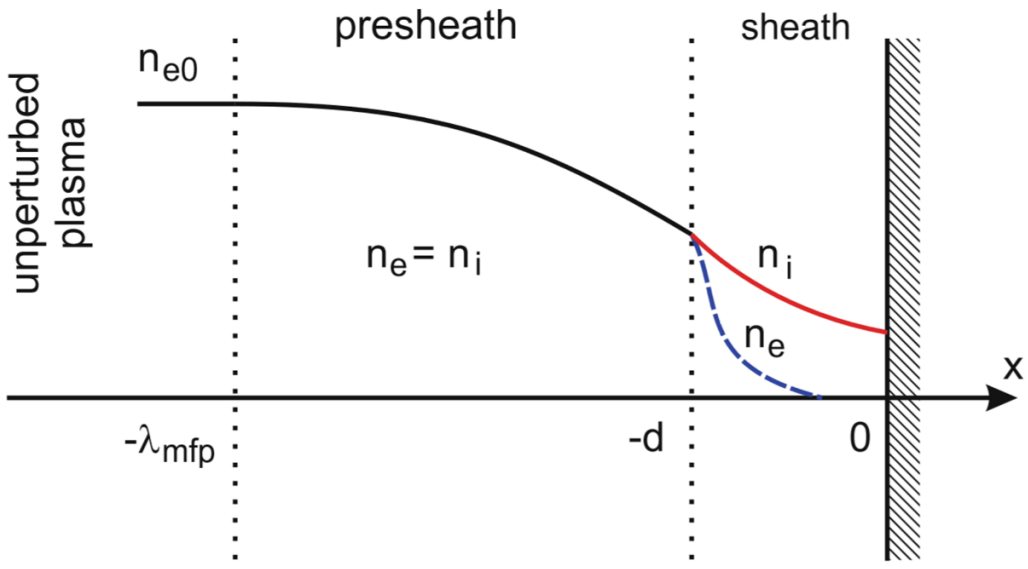

Figure 1 -Image showing the various regions that arise from the immersion of a probe in a plasma environment. Image taken from source [3].

seemingly useful expression for determination of the plasma sheath thickness, in practice, measurement of U is not typically straightforward. The equation however can be used as a means to estimate sheath thickness if one assumes a reasonable value for U, then using a measured current the ion current density may be calculated and used along the U to arrive at an estimated value for d which serves as a means to somewhat justify use of other theories to analyze the I-V characteristic gathered from the Langmuir probe measurements.

Looking once more to Figure 1, it shows that as the magnitude of the distance between the unperturbed plasma and the probe decreases the particle density also decreases. This means that if a measurement is made using the Langmuir probe, then the plasma density derived from the plasma I-V characteristic will not be representative of the unperturbed plasma density. Therefore, a relationship is needed to connect the plasma density derived from the I-V characteristic to that of the unperturbed plasma.

The relationship that we seek to fulfill the above connection is approximated by the results of the Bohm criterion. Once more, without a formal derivation, the Bohm criterion gives us that at the sheath edge the particle density is a fraction of that found in the unperturbed plasma. Equation (2.4) summarizes the approximation gathered from the Bohm Criterion. [3]

$$n_i(-d) = n_e(-d) = n_{e0} \exp\left(-\frac{1}{2}\right) \approx 0.61 n_{e0} \tag{2.4}$$

To summarize the Bohm Criterion, it is a result that drops out of an ion energy analysis near the sheath. The analysis seeks to establish conditions on the ion velocities that will result in a stable plasma sheath. That condition being that the velocity of the ions

at the sheath edge need to be greater than or equal to the Bohm velocity (v_B). Or equivalently stated by the inequality (2.5). [3]

$$u_0 \geq v_B = \sqrt{\frac{k_B T_e}{m_i}} \tag{2.5}$$

Having stated the above, if the Bohm criterion is satisfied then the theory predicts a stable sheath formation and thus (2.4) along with the obtained I-V plasma characteristic can be used to calculate a value for the unperturbed plasma particle density. In this study OML theory is used to calculate the plasma parameters of interest. The use of OML theory is discussed in a later.

For an ideal plasma I-V characteristic curve there are three distinct regions the I-V curve can be broken up into. Referring to Figure 2 below, region I is defined to be the ion saturation region. In this region there is a limit to how much ion current is drawn by the probe dictated by the condition at the sheath edge and stated mathematically by the Bohm criterion. The ion current into the probe will be proportional to the ion velocity at the sheath edge.

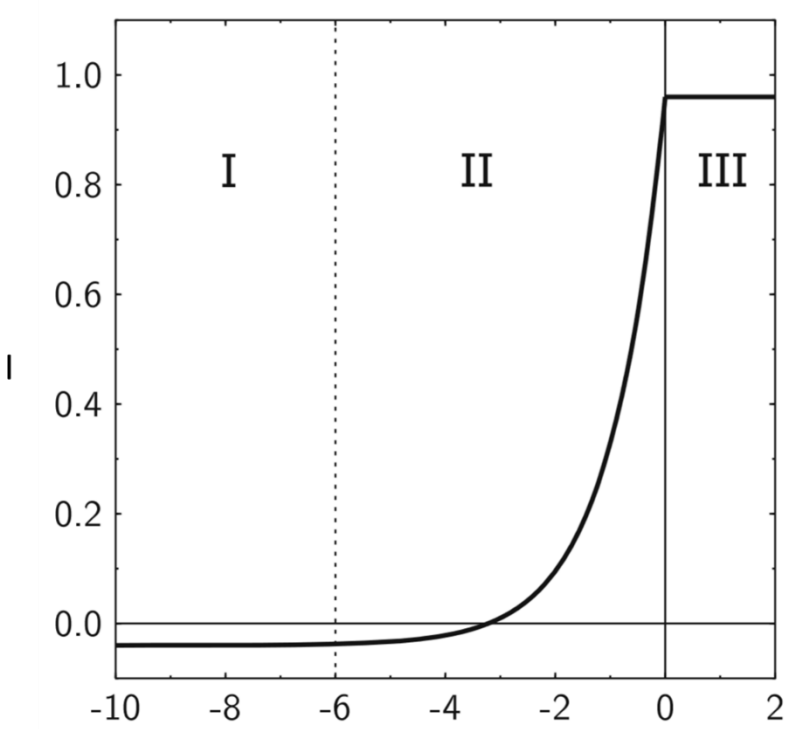

Figure 2 - Ideal I-V plasma characteristic curve showing the three regions of most importance.

Region II is the electron retardation region. In this portion of the I-V curve, the potential of the probe is increased to the point where ions or electrons no longer flow into the probe. This point is called the floating potential. Passed the floating potential, the electron current into the probe increases approximately exponentially. The slope of region II can be used to calculate electron temperature. [3] Region III defined in Figure 2 by were the potential is zero and onward is called the electron saturation region. More information on the three regions can be found in [2] and [3].

The experiment for which we built a Langmuir probe, forms an RF plasma in a cylindrical symmetry surrounding metal waveguides. The plasma itself acts as a waveguide and then microwave transmission measurements as described in the

introduction are performed. RF-generated plasma environments complicate probe design and data interpretation. RF signals interfere with the IV data collected by adding a sinusoidal signal onto the DC characteristics of the plasma. [4] Holding the probe at a fixed DC bias will inevitably cause a current flow between the probe and the plasma sheath formed around the probe due to the oscillating RF voltage. [4] The RF current cannot be used to determine plasma parameters because, in general the oscillating plasma potential is undetermined and so an I-V relationship is unobtainable. The effect of the RF voltage across the plasma sheath is to shift the floating potential of the probe to more negative values which in effect distorts the electron temperature values by making them unreasonably high and giving lower values than expected for the electron density. [4]

As mentioned, it is necessary to keep the fluctuations of the RF plasma from interfering with the I-V characteristics collected. If the effects of the RF fluctuations are not dealt with, calculations will give an unreasonably high electron temperature and values gathered for the plasma floating potential will be too low. [5] Of the techniques to prevent RF voltages from interfering with I-V measurements, the most effective has been to force the tip of the Langmuir probe to follow the RF plasma potential while simultaneously forming a low impedance path from the sensing circuitry to the plasma source. The way this is achieved is by use of tuned inductors and auxiliary floating electrodes. This RF compensation technique is referred to as passive RF compensation where passive circuit components are used to reduce the effects of RF on the measurement.

A high impedance to RF is achieved in a Langmuir probe by placing chokes as close to the probe tip as possible, along with a large enough floating auxiliary electrode

used to couple the plasma potential to the probe tip. [5] Using tuned chokes and an auxiliary electrode help to avoid the complicated behavior of a varying sheath capacitance in an RF plasma by coupling the fluctuating space potential to the probe tip and attenuating of the RF voltages at the measurement circuit. [5] The chokes and auxiliary electrode used need to be placed as close to the probe tip as possible to limit the amount of stray inductance and capacitance at 13.56 MHz. [5]

In describing passive compensation, a partially compensated probe is a good starting point to develop an understanding for RF probe compensation. With the partially compensated probe inner workings described, we can then move on to a discussion of a fully compensated probe. When designing an RF-compensated probe it is necessary to know the degree to which the probe couples to the plasma potential through the plasma sheath. [6] Chen mentions that to estimate the capacitive coupling of a probe, one should assume that the plasma sheath formed around the probe is a vacuum capacitor whose thickness can roughly be estimated. [6]

An equivalent circuit that models a partially compensated probe can be seen in Figure 3. Illustrates the sheath capacitance formed between the plasma and the probe tip. In Figure 3 the probe tip is given by the node at P, C_{sh} is the coupled sheath capacitance

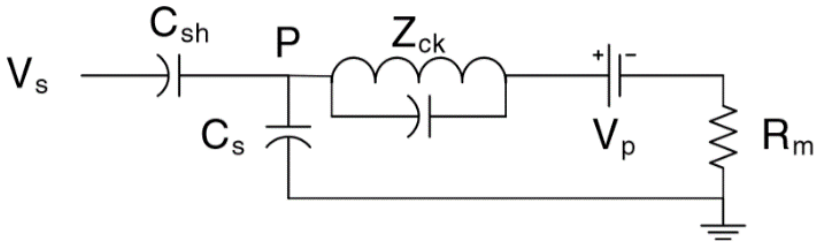

Figure 3 - Equivalent circuit for a partially compensated probe.

formed between the probe and the plasma that is at the space potential given by V_s.

The portion of Figure 3 with the inductor symbol in parallel to the capacitor symbol represents inductors strung together in series and their stray capacitances with an impedance given by Z_{ck}. [6] Ideally, the chokes are of high enough impedance and resonate at the RF frequency used that they filter out the RF potential from reaching R_m, the resistor used to measure current flowing through the probe. R_m is connected to a supply voltage given by V_p that applies a DC bias on the probe tip and whose current supplied is essentially invisible to the chokes. To simplify this analysis further, assume that R_m is small enough that it may be neglected. The probe tip then approximately fluctuates at the sheath edge potential V_{sAC}. [6] Any voltage applied by the DC supply will then raise the probe tip to that DC potential causing there to be a potential difference between the probe tip and the fluctuating plasma. Further assuming that the stray capacitance between the probe tip and the system ground is negligible then C_{sh} and Z_{ck} form a voltage divider for AC signals whose potential at point P in Figure 3 can be modeled by

$$V_{pAC} = V_{sAC}\left(\frac{Z_{ck}}{Z_{ck} + Z_{sh}}\right) \tag{2.6}$$

where Z_{sh} is the impedance of the sheath. From (2.6) we see that when $Z_{ck} \gg Z_{sh}$ then the probe voltage is approximately equal to the AC plasma potential. [6] Chen says in [6] that in order for the I-V characteristics collected by the compensated probe to be unaffected by RF pickup (2.7) is a requirement,

$$\left(\frac{e}{KT_e}\right)\left(V_{sAC} - V_{pAC}\right) \ll 1 \tag{2.7}$$

And so when the choke impedance is much greater than the sheath impedance, the sheath edge potential is approximately equal to the RF pickup $V_{sAC} \approx V_{RF}$. A further approximation can be made that can be used to derive an order of magnitude difference between the sheath and choke impedance. This relationship is given by,

$$\frac{eV_{RF}}{KT_e}\left|\frac{Z_{sh}}{Z_{ck}+Z_{sh}}\right| \approx \frac{eV_{RF}}{KT_e}\left|\frac{Z_{sh}}{Z_{ck}}\right| \ll 1 \tag{2.8}$$

From (2.8) above the choke impedance can be calculated by using the following equation from [7] that gives the DC sheath capacitance as a function of the difference between DC sheath and probe potentials

$$C_0 = \frac{A_p}{2^{\frac{5}{4}}}\frac{\epsilon_0}{\lambda_D}\left[\frac{e\left(V_{sDC}-V_{pDC}\right)}{KT_e}\right]^{-\frac{3}{4}} \tag{2.9}$$

where A_p is the probe surface area and λ_D is the Debye length. These estimates can be carried out by assuming values for $V_{sDC} - V_{pDC}$ as well as the KT_e. The sheath impedance can then be found at the RF frequency used (13.56 MHz) in the equation $Z_{sh} = -\frac{j}{2\pi f C_0}$. Using this strategy gives an estimate of the choke impedances needed for RF compensation of the probe.

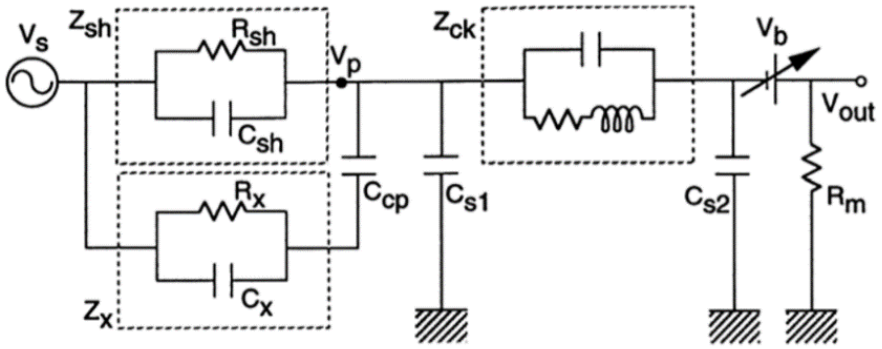

Figure 4 - schematic diagram of a fully compensated Langmuir probe. Image from reference [6].

Remembering that for the analysis above, that of a partially compensated probe, the stray capacitance between the probe tip and ground was omitted to derive the voltage divider relationship. We now include its effects and derive expressions for calculating choke impedances as well as surface areas for auxiliary electrodes for fully compensated probes. The schematic diagram for a fully compensated probe is given by Chen in [6] and presented here as Figure 4. In Figure 4 V_s is the plasma space potential, V_p potential at the probe tip, V_b is used to denote a variable DC bias supply that is used to raise or lower the voltage at the probe tip relative to the plasma space potential and V_o here is the output of the circuit used to measure the current that is flowing through a resistor R_m connected to ground. The circuit components within the dashed boxes represent the impedances seen from the plasma looking into the probe. Z_{sh} as before stands for the sheath impedance modeled by a parallel combination of a resistor (R_{sh}) and a capacitor (C_{sh}). Z_x here stands for the impedance of the auxilary electrode used to couple the fluctuating plasma potential to the probe tip through a coupling capacitor (C_{cp}). Z_x similar to Z_{sh} is modeled by a parallel combination of a resistor (R_x) and a capacitor (C_x). The choke impedances are then given by Z_{ck} whose equivalent circuit diagram is given by a resistor in series

with an inductor both in parallel to a stray capacitance intrinsic to the inductor coils used. Lastly, C_{s1} stand for a stray capacitance that arises between the wire that connects the probe tip to the chokes and the walls of the probe and C_{s2} is the stray capacitance of external circutry used to make the measurement. The labels for Figure 4 were gathered from Ref. [7].

The RF chokes are designed to have a resonance at the first and second harmonic of the RF frequency used (13.56 MHz and 27.12 MHz). Along with that specification, care must be taken to choose chokes that are small enough to fit in the probe while having a large enough Q factor to give the needed impedance. [7] The stray capacitance formed between the probe tip and the the housing of the Langmuir probe connected to ground effectively decreases the impedance of the chokes. Z_{ck} is in parallel with the the impedance of the stray capacitance $Z_{s1} = -\frac{j}{2\pi f C_{s1}}$. If this drop in impedance is great enough to make (2.8) no longer true, then the true I-V characteristis of the plasma will not be resolved. To eliminate this problem, an auxiliary electrode needs to be placed as close to the probe tip as possible with the following realtionship between the probe tip area and the electrode area holding true,

$$A_x \gg A_p \tag{2.10}$$

where A_x is the surface area of the auxiliary electrode and A_p is the probe tip surface area. [7] The coupling capacitor (C_{cp}) used needs to be big enough to alow the RF signals coming from the plasma to pass through with little attenuation while still being small enough so that it looks like an open circuit to low-frequency signals. When the previous requirements are met, the auxiliary electrode drives the probe tip at the RF of the plasma.

[7] The condition that must be satisfied to get the probe tip to be driven by the RF plasma source is,

$$Z_c \gg Z_x \left(\frac{e|V_{RF}|}{KT_e} - 1 \right) \tag{2.11}$$

where Z_c is the smaller impedance between Z_{ck} and Z_{s1}. [7]

Langmuir probes are inserted into a plasma and a bias potential is swept between a negative to positive voltage (usually a triangle wave) to collect electron and/or ion current that is then sourced across a current sense resistor. [8] Ohm's law can then be used to calculate the current passing through the resistor of known value if the voltage drop across the resistor is measured.

The two plasma parameters of most interest to the researchers the experiment descirbed in the introduction are the plasma electron density (n_e) and the electron temperature (T_e). Mathematical relationships are needed that relate the two previously mentioned plasma parameters to the characteristics of the I-V curve generated by the probe. In the Experiemenal Results and Procedure section, orbital motion limited (OML) theory will be used to calculate the value of interest. Refer to the section for more information on the subject of calculating n_e and T_e.

III. PROBE DESCRIPTION

In the discussion that follows, a detailed description of the Langmuir probe built for the mentioned study is given. The probe was built around the schematic given by Sudit and Chen. [7] To summarize what follows, the probe can be broken down into three distinct sections, the first being the front end of the probe, or what is immersed into the plasma. The second section is the middle of the probe where the RF compensation circuitry is contained and lastly, the backend of the probe is where the sensing circuitry (to be discussed in a later section) is connected to a port to make a measurement.

In Figure 5 below, there is a 3-D model of the completed Langmuir probe showing all three sections mentioned above. The front end is found in the lower left-hand corner and the rest of the sequence can be deduced from the given information.

Figure 5 - 3D CAD model of Langmuir probe built for the mentioned experiment. Isometric view.

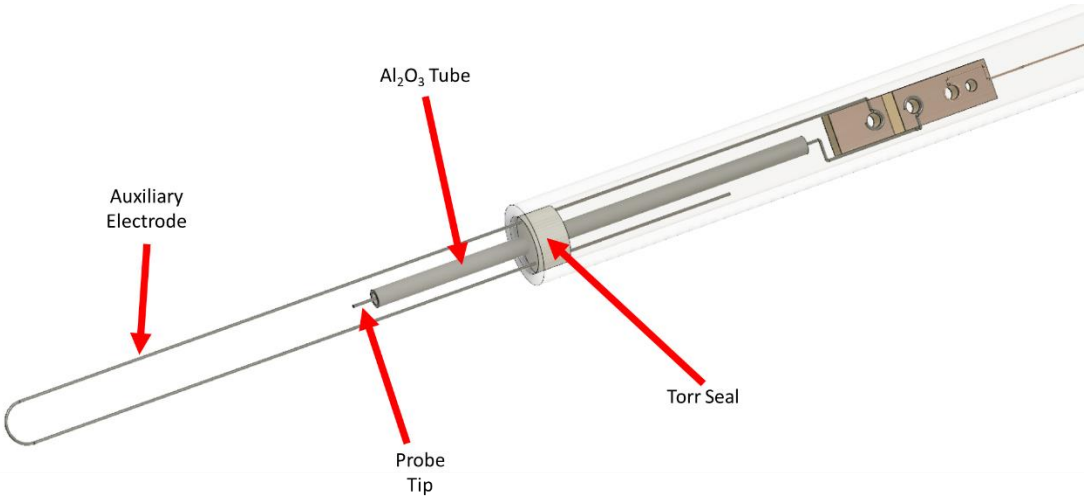

Figure 6 - Front-end of Langmuir probe showing auxiliary electrode, probe tip, Al2O3 tube and Torr Seal.

The front end of the probe shown in Figure 6 consists of the auxiliary electrode, probe tip, alumina (Al_2O_3) tube that houses the probe tip, and an epoxy material (Torr Seal) used to hold the assembly in place but not to make a vacuum seal in the front end.

The auxiliary electrode is constructed out of 0.3 mm-diameter tungsten wire bent into a semi-circular shape at the furthest end of the probe. As mentioned in the theory section, the auxiliary electrode serves to couple the oscillating plasma potential to the probe tip so that a DC bias imposed on the tip will draw a direct current from the plasma while eliminating interfering alternating RF current. The probe tip is made out of the same 0.3 mm-diameter tungsten wire that the auxiliary electrode is made of and is fed through a 1.6 mm OD, 1 mm ID alumina tube used to shield the probe wire from the plasma except for the tip that protrudes out of the end as seen in *Figure 6*. Holding the three components mentioned above in place, while providing a port for air to be evacuated from the quartz tube, is Torr Seal, a two-part low vapor pressure epoxy that solidifies when mixed. Although Torr Seal is intended to form a vacuum seal in low

pressure systems, in the front end of the probe it is simply used as a method of rigidly adhering the front-end components in place. Further specifications on dimensions can be found in the 2D diagrams. Refer Figure 11 for a 2D schematic of Langmuir probe.

The middle of the probe houses a small double-sided copper clad circuit board with four holes drilled into it. Figure 7 shows the front side of the middle portion of the probe. For viewing purposes, the screws used to hold the wires down to the PCB have been omitted.

These screws are fastened into the holes drilled on the PCB. In Figure 7 it can be seen that the tungsten wire used to form the auxiliary electrode and the probe tip have been bent into a partial circular shape and placed concentric with their respective drilled holes. Screws are then used to hold the bent tungsten wire to the PCB making an acceptable electrical connection. The same is done to the copper wire used to connect the

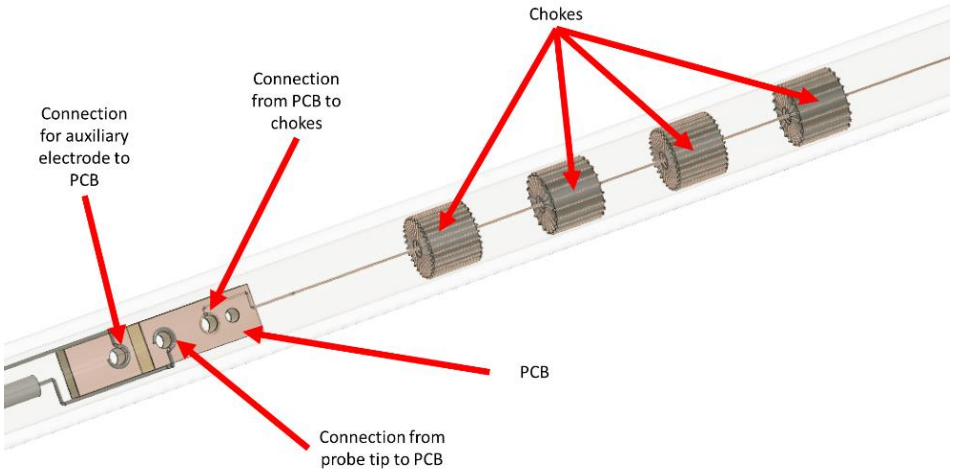

Figure 7 - Middle section of the probe showing the front side. The actual probe takes screws in the holes for connecting the wires to the PCB but they have been omitted here for viewing purposes.

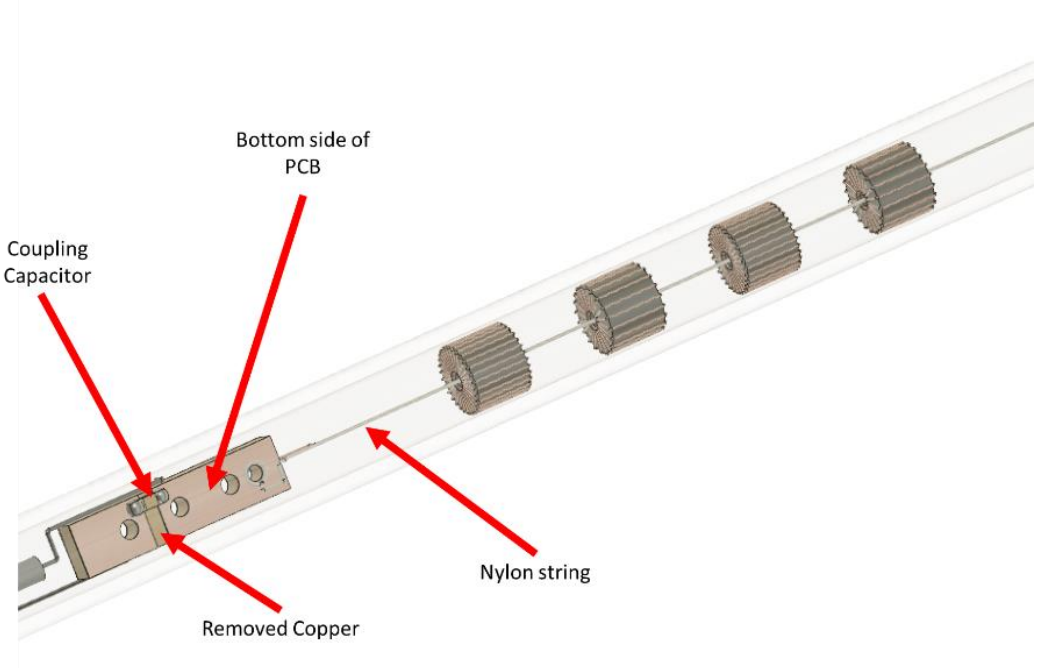

Figure 8 - Bottom side of middle section of Langmuir probe showing the coupling capacitor, and a nylon string used to keep the chokes taut in place.

PCB to the chokes. Figure 8 shows the bottom side of the middle section which shows a soldered-on surface mount capacitor (10 nF) bridging a gap between the port that connects the auxiliary electrode to the probe tip/chokes. Figure 8 also shows another hole drilled to the far right of the PCB. This hole can be used to either take a screw to hold a piece of nylon string or simply can be used to tie a piece of nylon string to. The nylon string is wrapped around each of the four chokes and then is held down in place at the end of the probe with Torr Seal epoxy. The nylon string serves to keep the chokes taut in place and limits their range of motion which can cause the solder joints between them to weaken and break. Also, unwanted electrical shorts may occur if the chokes are not held rigidly in place. Another detail to notice is that on both the top and bottom of the PCB there is a section of the copper clad board that has been removed between the first and the second holes closest to the left-hand side of either Figure 7 and Figure 8. This removed

section is there to create an electrical isolation between the auxiliary electrode and the node on which the probe tip and chokes are on.

Lastly, the back end of the probe can be seen in Figure 9. The main components of the back end of the probe are the signal breakout pin used to connect the sensing circuitry to the probe (see next section for discussion of circuitry). The breakout pin was taken from a DIP IC socket and a simple solder joint was made between the copper wire and the pin. The next component of the back end is a loop made of 1.63 mm solid core

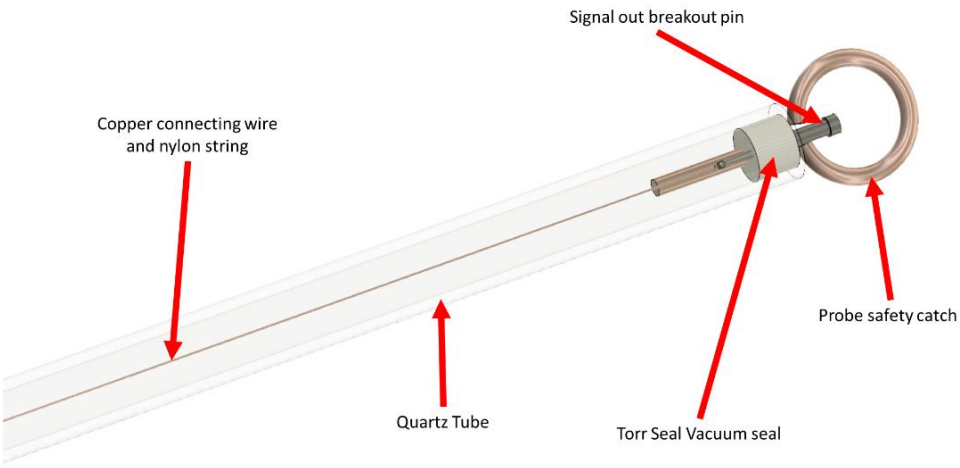

Figure 9 -Back-end of Langmuir probe showing the safety catch and a breakout pin for connecting to sensing circuitry.

copper wire bent into the shape of a loop of a diameter of 10.6 mm. The loop diameter is not critical. However, it should be large enough so that if the probe were to be improperly installed in the probe pass-thorough assembly the copper loop would restrict the probe from being completely sucked into the chamber. Lastly, the two components mentioned previously as well as the nylon string mentioned earlier are all secured in place by Torr Seal epoxy which also serves to form a vacuum seal at the back end of the probe.

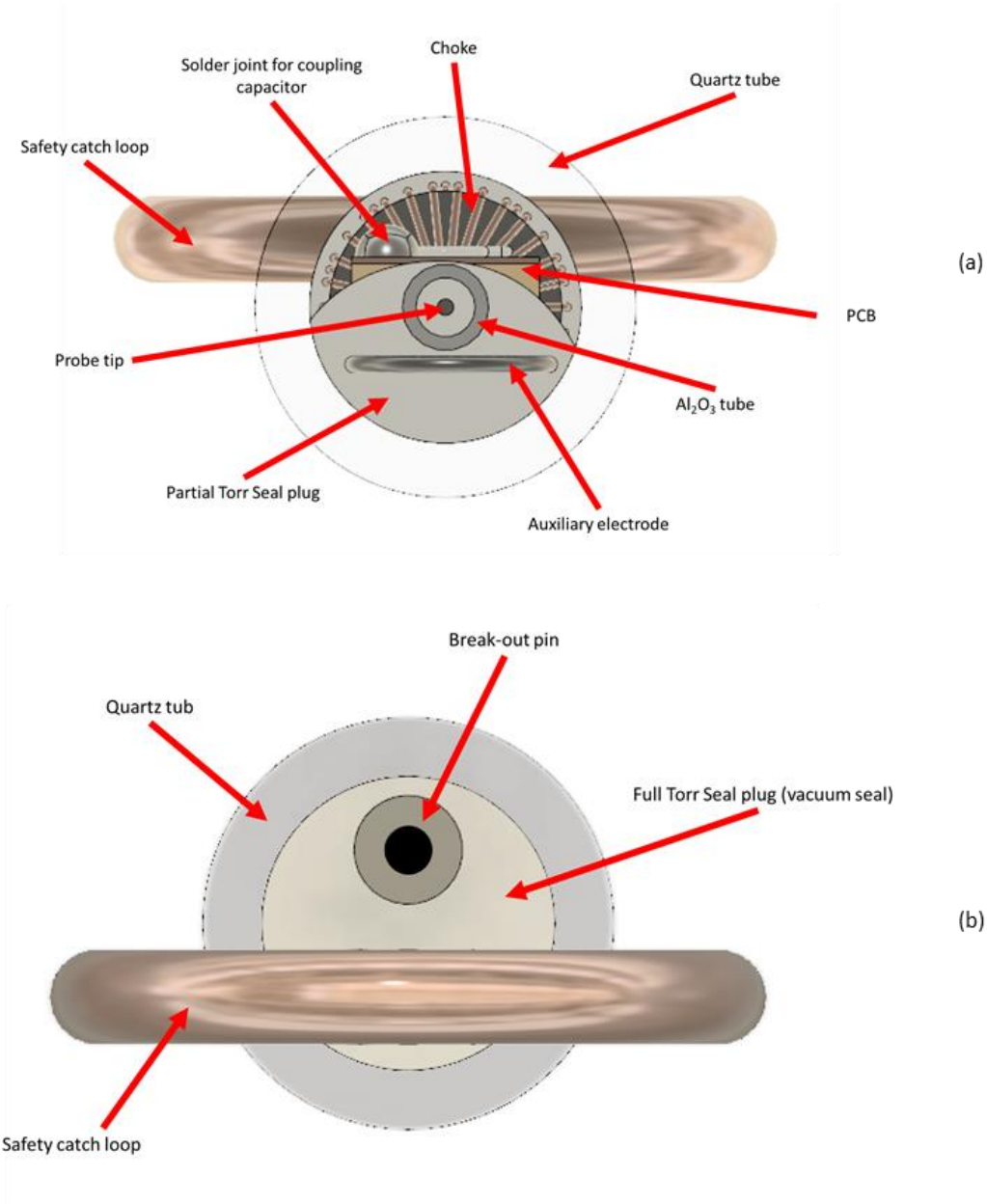

Figure 10 - (a) Bottom view of Langmuir probe, (b) top View of probe.

Up to this point, all views of the probe have been presented except for a top and bottom views. For the reader interested in constructing a replica of this probe, Figure 10 gives the last two remaining views of the probe.

Figure 5 through Figure 10 show what the Langmuir probe should look like once it has been constructed but these figures lack the specific physical dimensions needed to

actually build a replica of the probe used for our experiments. With, what follows is a 2-D schematic drawing of the probe with the quartz tube and views of the front, back, top and bottom. Refer to Figure 11 for 2-D schematic drawing of the probe.

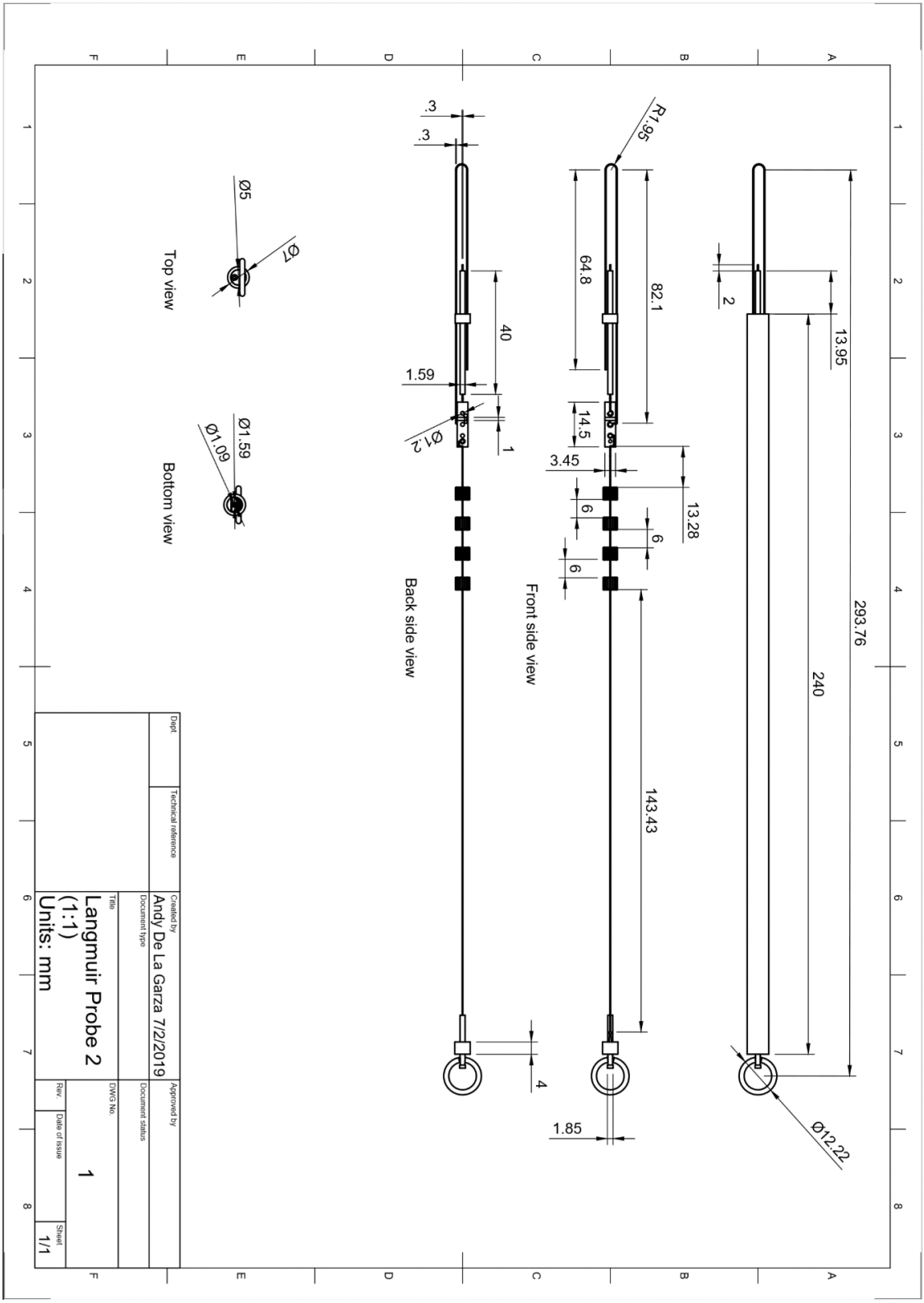

Figure 11 -2-D schematic drawing of Langmuir probe with physical dimensions.

IV. CONSTRUCTION OF PROBE DRIVER CIRCUIT

In the following sections the sensing circuitry used in this experiment is discussed. However, before the circuit used to generate an I-V plasma curve is discussed in more detail, an overall functional block diagram of the system in which the sensing circuitry is used serves to guide the reader in understanding how it fits into the system as a whole. With that being said, consider Figure 12. Figure 12is a functional block diagram of the Langmuir probe IV measurement system showing all major components needed to make our particular set-up work. Starting from the upper left-hand corner of Figure 12 we derive power from a standard wall outlet that is hooked up to an isolation transformer, a DC lab bench power supply (Aim TTi EL561R Power Supply) and, an arbitrary waveform generator (GW INSTEK AFG-2125). The isolation transformer was used to reduce 60 Hz noise coming for mains voltage supply that was showing up in the data

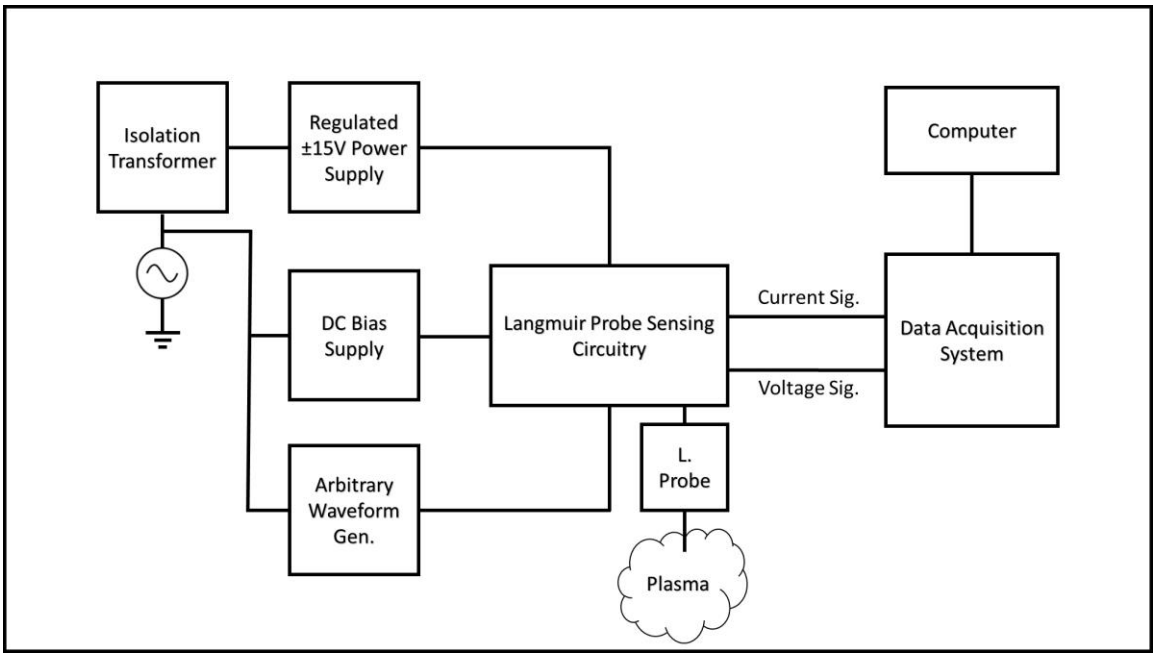

Figure 12 - Functional block diagram of the Langmuir probe measurement system.

collected by the sensing circuitry.

The filtered AC voltage from the isolation transformer is then connected to a DC ±15V linear regulated power supply circuit. The outputs of the linear regulators are then connected to an output terminal labeled SV1 in Figure 13. The ±15V supply circuit schematic can be seen in Figure 13. The supply consists of two sets of ±15V supplies

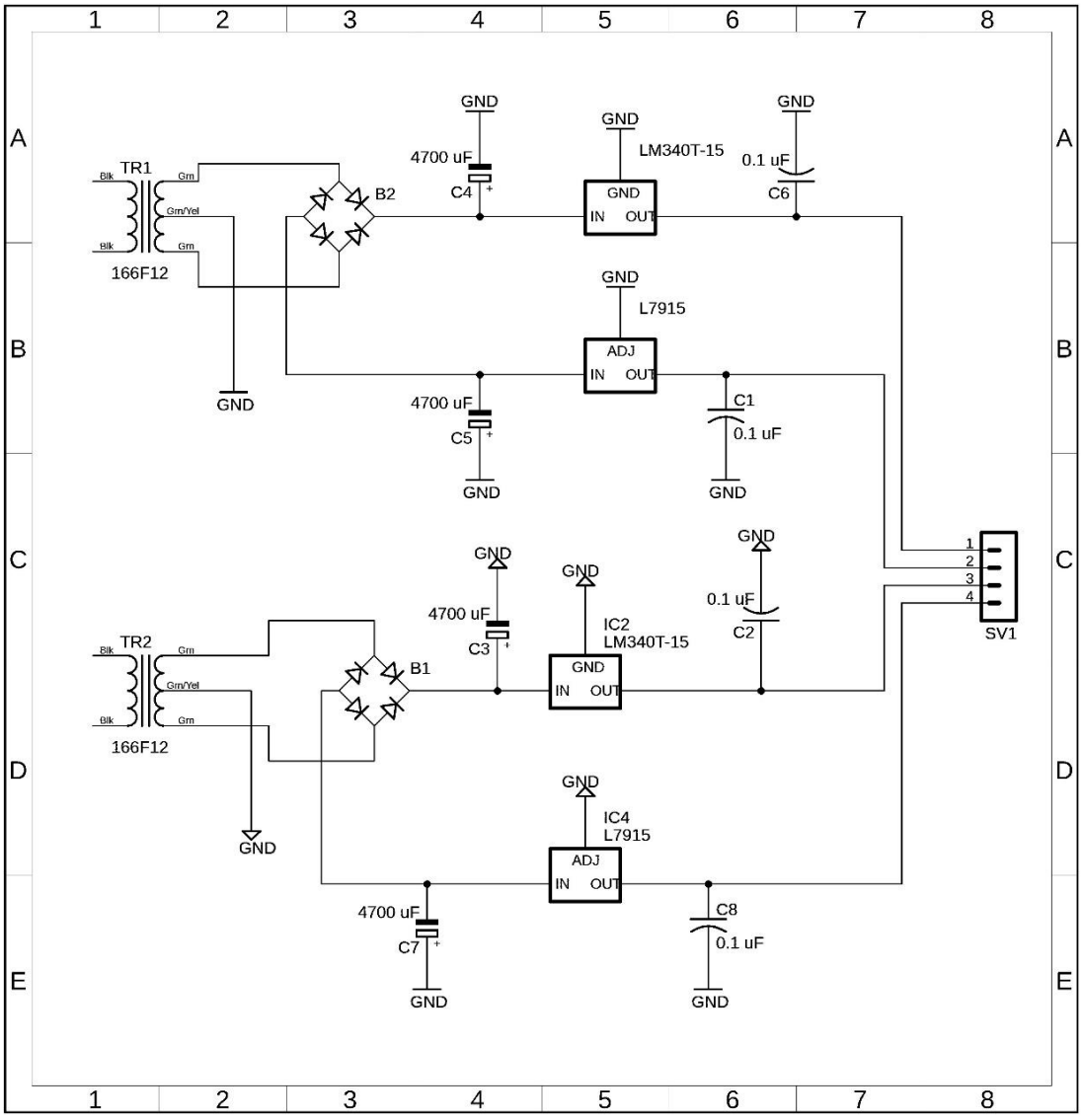

Figure 13 - Circuit schematic of ±15V linear regulator power supply.

referenced to different ground potentials. The regulated ±15V that is connected to pin 1 and 2 on SV1 in Figure 13 is referenced to a lab ground or the ground that everything in the system as a whole is connected to. The lab ground is depicted by a flat bar labeled GND in the figure. On the other hand, the ±15V that is connected to pins 3 and 4 on SV1 in Figure 13 is referenced to a local ground connection that is symbolized in the figure by a triangular ground symbol. The reason for the two ±15V supplies will become apparent when the Langmuir probe sensing circuity is discussed. Taking a look back at Figure 12, the two boxes below the power supply are the DC bias supply and the arbitrary waveform generator.

The DC bias supply serves to raise the Langmuir probe tip potential to a varying voltage in the range of ±50 volts. With the probe tip bias set the arbitrary waveform generator then sends a 20V signal peak to peak (triangle wave) to the sensing circuit that then raises and lowers the potential of the probe tip around the set DC bias. Another look to Figure 12 shows that the power supply, DC supply and function generator are all connected as inputs to the Langmuir probe sensing circuitry. The last input to the sensing circuitry is the Langmuir probe itself which is depicted as being immersed in the plasma. Finally, a voltage signal for the probe voltage and the probe current goes from the Langmuir probe circuit to an NI-cDAQ9133 data acquisition system for collecting data which can then be transferred to a personal computer for analysis.

Now that the Langmuir probe system has been presented in a simplified functional block diagram, we can expand on the Langmuir probe sense circuitry beginning with a functional block diagram of the circuit itself to gain a general understanding of all the stages found within the circuit. Refer to Figure 14 for the functional block diagram.

This time starting from the right-hand side, there are two boxes representing the power into the circuit. There is a DC bias referenced power supply that powers various components within the circuit. This supply is connected to the plus and minus terminals of the external DC power supply. The other supply is of a lab ground referenced supply that comes from the linearly regulated power supply.

Above the power supply boxes there is a box labeled Probe Voltage Driver. This stage takes a signal from the waveform generator and follows the potential of the signal

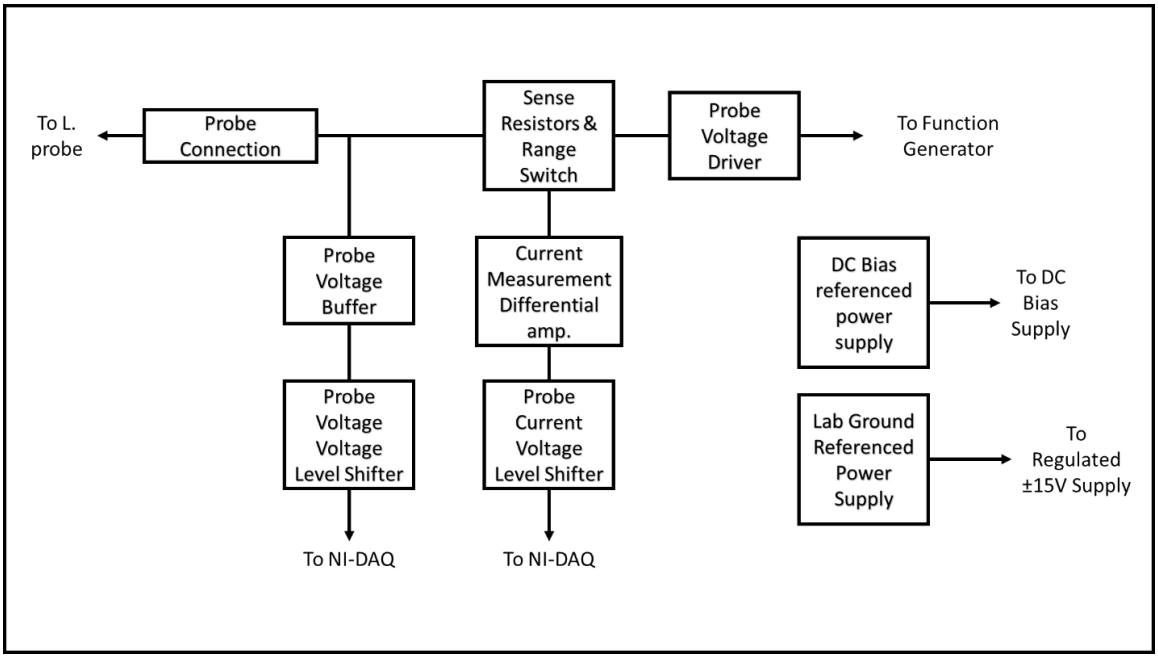

Figure 14 - Functional block diagram of Langmuir probe sense circuitry.

driving the probe tip. Before the probe tip there is a series of current sensing resistors, labeled Sense Resistors & Range Switch, whose terminals are connected in parallel to a differential amplifier stage called the Current Measurement differential amp. The differential amplifier stage is used to measure the voltage drop across the resistors. This voltage drop across the selected resistor range can be used to calculate current into or out of the probe. This is done in the buffer stage seen below the differential amplifier stage called Probe Current Voltage Level Shifter. On the probe side of the sensing resistors is a buffer stage, here called the Probe Voltage Buffer that follows the probe voltage and feeds it to a calibrating stage that subtracts off the DC bias from the probe potential, here called the Probe Voltage Voltage Level Shifter. As seen in Figure 14 the outputs of the Probe Voltage and Current Voltage Level Shifters are connected to the NI-cDAQ9133. Now equipped with a general understanding of the probe circuit, we can look to the actual circuit schematic and discuss the functions of the various components.

The design for the Langmuir probe sense circuit was taken from an undergraduate physics laboratory handout in plasma physics. [9] The circuit schematic was redrawn in a free version of Autodesk Eagle (PCB design software) and had to be broken down into two individual circuit boards because the free version of the software has a restriction on how large the area of a board layout can be. The complete circuit schematics are shown in Figure 15 and Figure 16.

Figure 15 is one of two circuit board schematics made for the Langmuir probe sensing circuit board. This first board, starting from the top left-hand corner, has a male

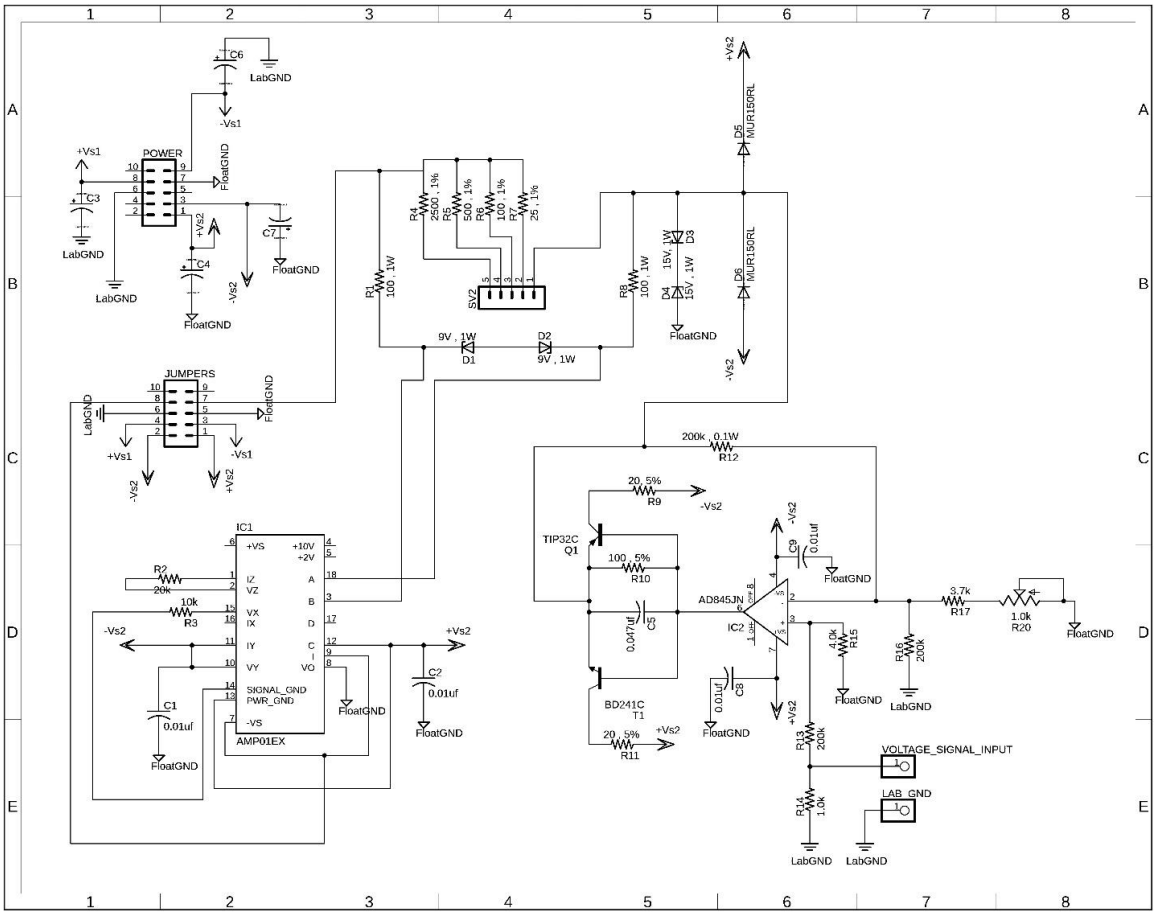

Figure 15 - Part 1 of 2 of the Langmuir sense circuitry. This circuit schematic contains the layout for the probe driver, sensing resistors and, instrumentation amplifier as well as a port where jumper's wires can be used to power and send signals to the second board.

pin header connector labeled POWER where an external power supply (mentioned earlier) is connected to and powers the board. Below the POWER connector symbol there is another similar connector symbol labeled JUMPERS. This connector is used to connect the power supply and signals coming from the first board to the second board. Below and to the left of the JUMPERS symbol we have the connections to be made to the AMP01EX instrumentation amplifier that precisely measures the voltage difference across the sensing resistors labeled R4 – R7. Hookup wire and a switch can then be used to change the resistor used to measure current flow through the probe tip by completing a connection between pin 1 on SV2 and any other pin on SV2. Lastly, in the bottom right hand corner of Figure 15 is the probe driver circuit with appropriate voltage level shifting. This stage receives a signal from the waveform generator and superimposes that signal onto the DC bias supply so that it can drive the Langmuir probe tip about the DC set bias.

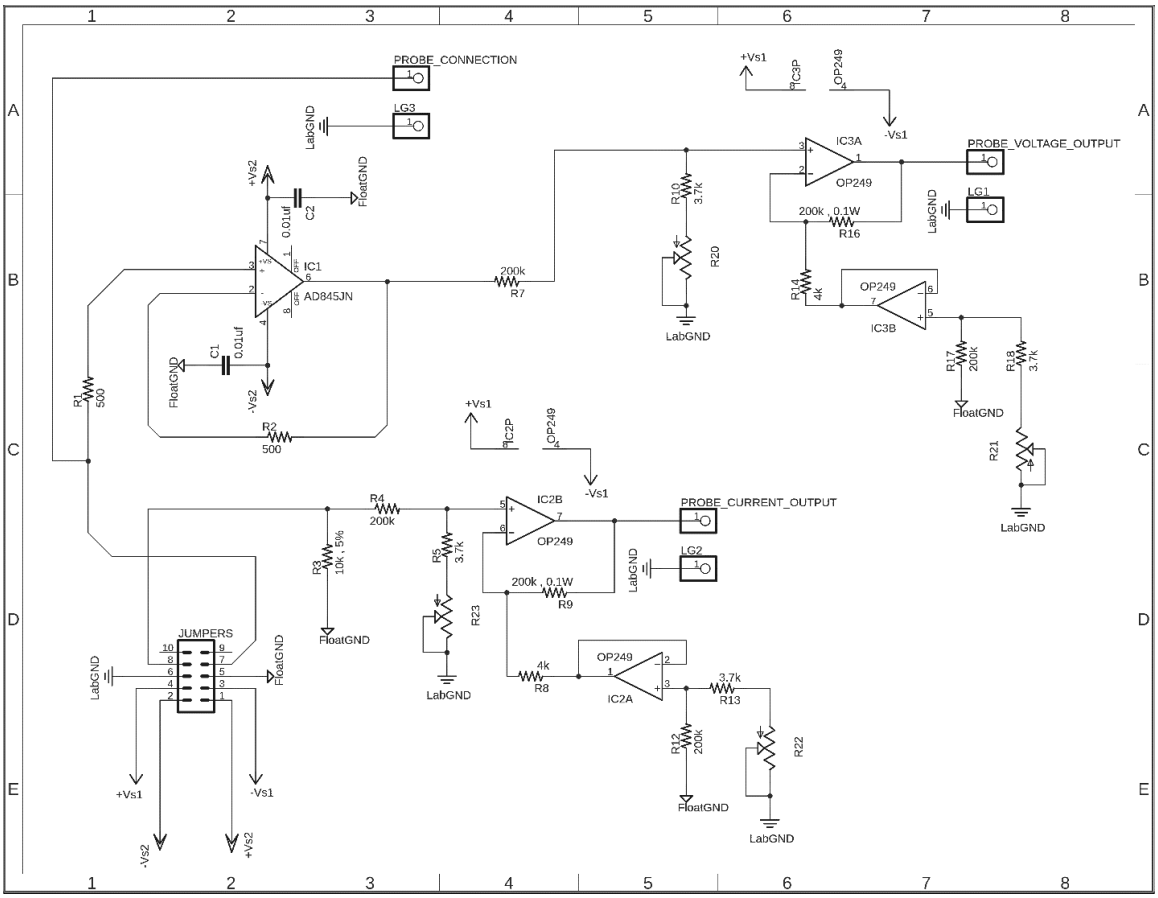

Figure 16 - Part 2 of 2 for Langmuir probe sense circuitry. This board shows the voltage buffer stage for the probe voltage, its respective voltage level shifter, and the voltage level shifter for the probe current circuit, as well as a port for jumpers to jump power and signals from the first board to the second board.

Figure 16 is the schematic diagram of the second part of the Langmuir probe circuit board. In this schematic starting from the lower left-hand corner is the symbol labeled JUMPERS. Using an AMP ribbon cable connector and 10 wire ribbon cable, power and other voltage signals from the first connect to the second board. Above the JUMPERS schematic symbol is a AD845JN op-amp configured as a voltage buffer used to sample the voltage of the probe tip. The buffer follows the voltage signal of the probe and sends it to a level shifter dual op-amp circuit labeled the OP249. Lastly, the

JUMPERS connect the output of the instrumentation amplifier on the first board to a voltage level shifter on the second board depicted here as IC2 (A and B). The output of this stage is a voltage signal that is proportional to the current flowing through the Langmuir probe.

One last detail about the two circuit schematics given above (Figure 15 and Figure 16): all the inputs and outputs on the boards have a system ground connection close by. The connection to ground is used to connect the shield on a BNC connector to protect the signals from being corrupted by stray voltages.

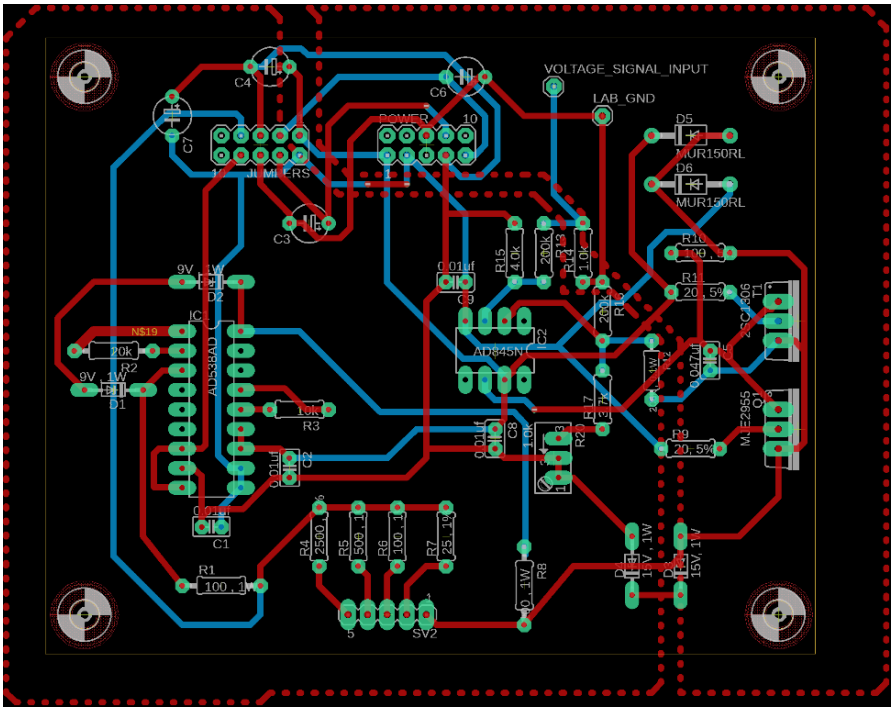

Figure 17 - PCB layout for board 1 of 2. This board layout corresponds to the schematic in Figure 15. Red lines are copper traces on the top layer, blues lines are copper traces on the bottom layer. The hashed red lines correspond to areas on the board where there is a copper ground plane.

As discussed above, the two circuit boards that make up the Langmuir sense circuit board were modeled in a free version of Autodesk Eagle. The PCB layout was also designed in the software. Figure 17 shows the layout of the PCB that is derived from the schematic in Figure 15. The red lines represent copper traces on the top layer of the board and the blue lines are representative of copper traces on the bottom of the board. All dashed red lines forming polygons indicate area that is to be filled with copper pour for a ground plane. The polygon formed on the left-hand side was chosen to be connected to the local ground and the polygon on the right-hand side was chosen to be connected to the lab (system) ground. Figure 18 shows the PCB layout for part 2 of the Langmuir sense circuit board. The red and blue lines in this layout have the same meaning as in the first board. For this board, the polygon formed by the dashed lines on the right-hand side is connected to local ground and the polygon formed on the left-hand side is connected to the lab (system) ground.

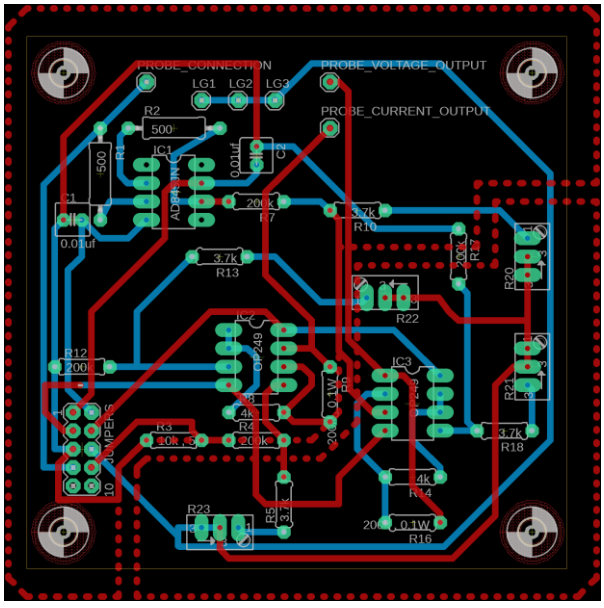

Figure 18 - PCB layout for board 2 of 2. Again, red lines indicate copper traces on the top plane and blue lines copper traces on the bottom layer.

The two PCB layouts above were exported as CAM files and were uploaded to the JLCPCB PCB manufacturing company website for fabrication of the boards. Once the boards arrived the components in the above schematics were soldered in. A Hammond Manufacturing ® metal enclosure was chosen to house the two boards was modified to take bolts to hold the boards along with a shaped piece of acrylic to keep the solder joints on the bottom of the circuit boards from making a short to the grounded

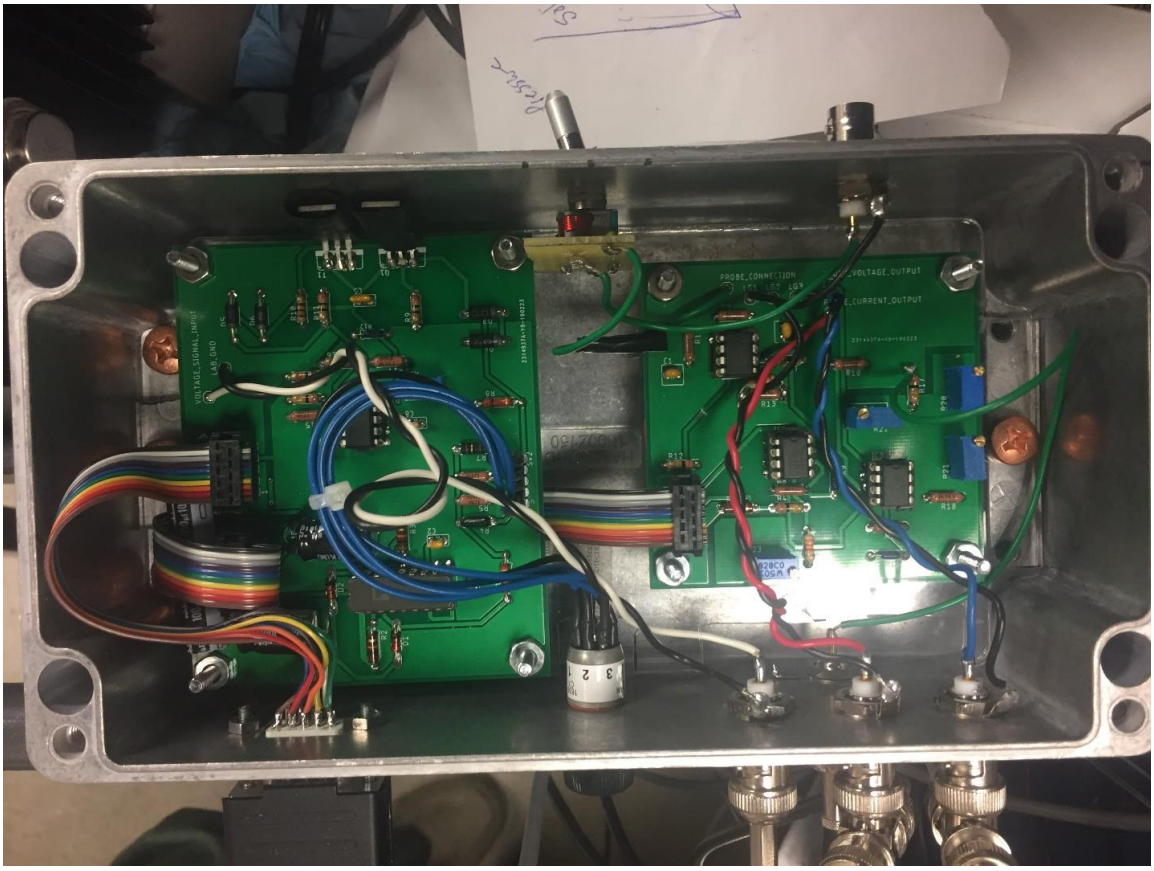

Figure 19 - Inside of the grounded metal box used to shield the Langmuir probe sense circuitry.

metal box. Figure 19 is a picture of the interior of the Langmuir sense circuitry in its shielded metal container. In the lower right-hand corner of this figure the BNC connections can be seen. The one furthest from the right is the connection to the signal generator, the middle connection is the voltage output, and the one furthest to the right is the current signal output. Below the three outputs is the DC bias input. Off to the left of the four BNC connectors previously discussed is the range switch, that is used to select the current sense resistor. Further to the left is the sub-D9 connector connecting to an external power supply. At the top of Figure 19 there is a switch that is in series with a

fuse and a choke used to attenuate RF voltage from interfering with the sense circuitry. To the right of the switch is a BNC connector that is meant to be connected to the Langmuir probe. Below Figure 20 – 23 provide more views of the Langmuir probe sensing circuitry box.

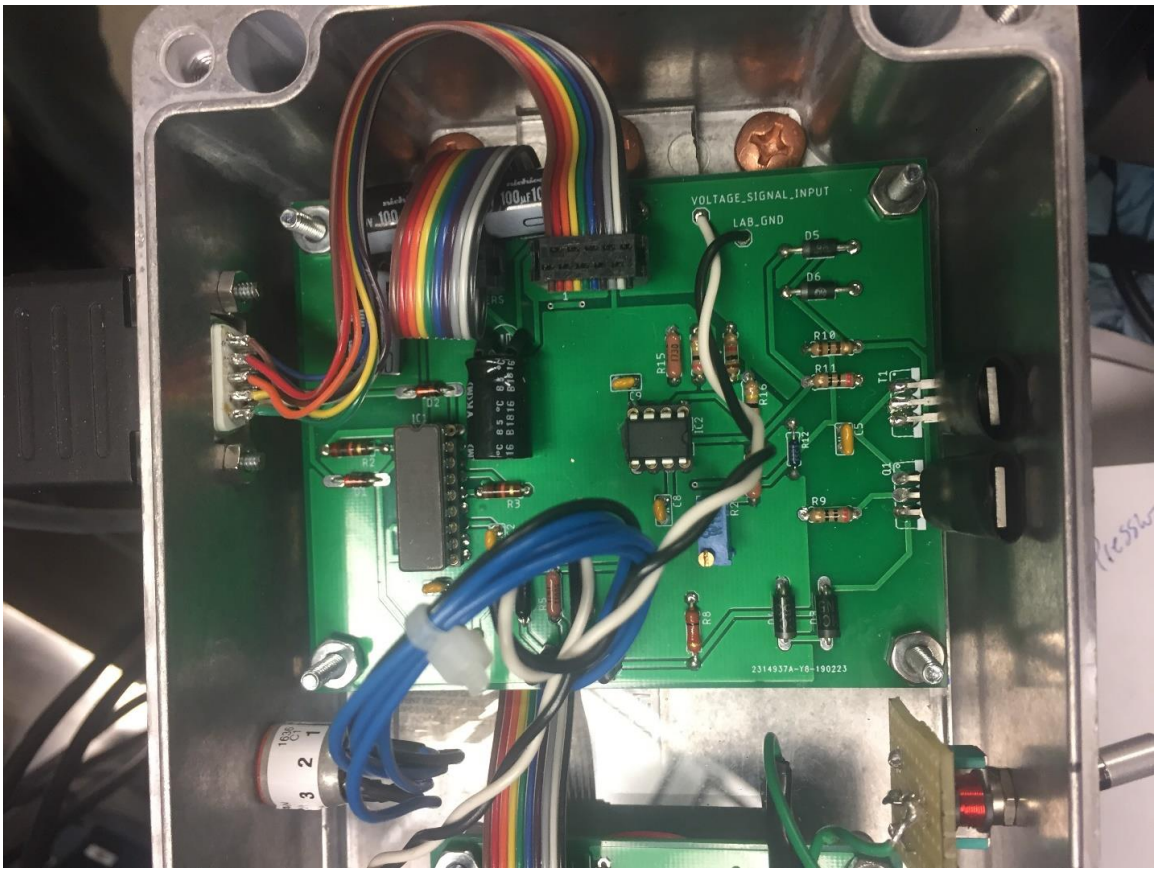

Figure 20 - Closer view of the first of the two boards that make up the sense circuitry.

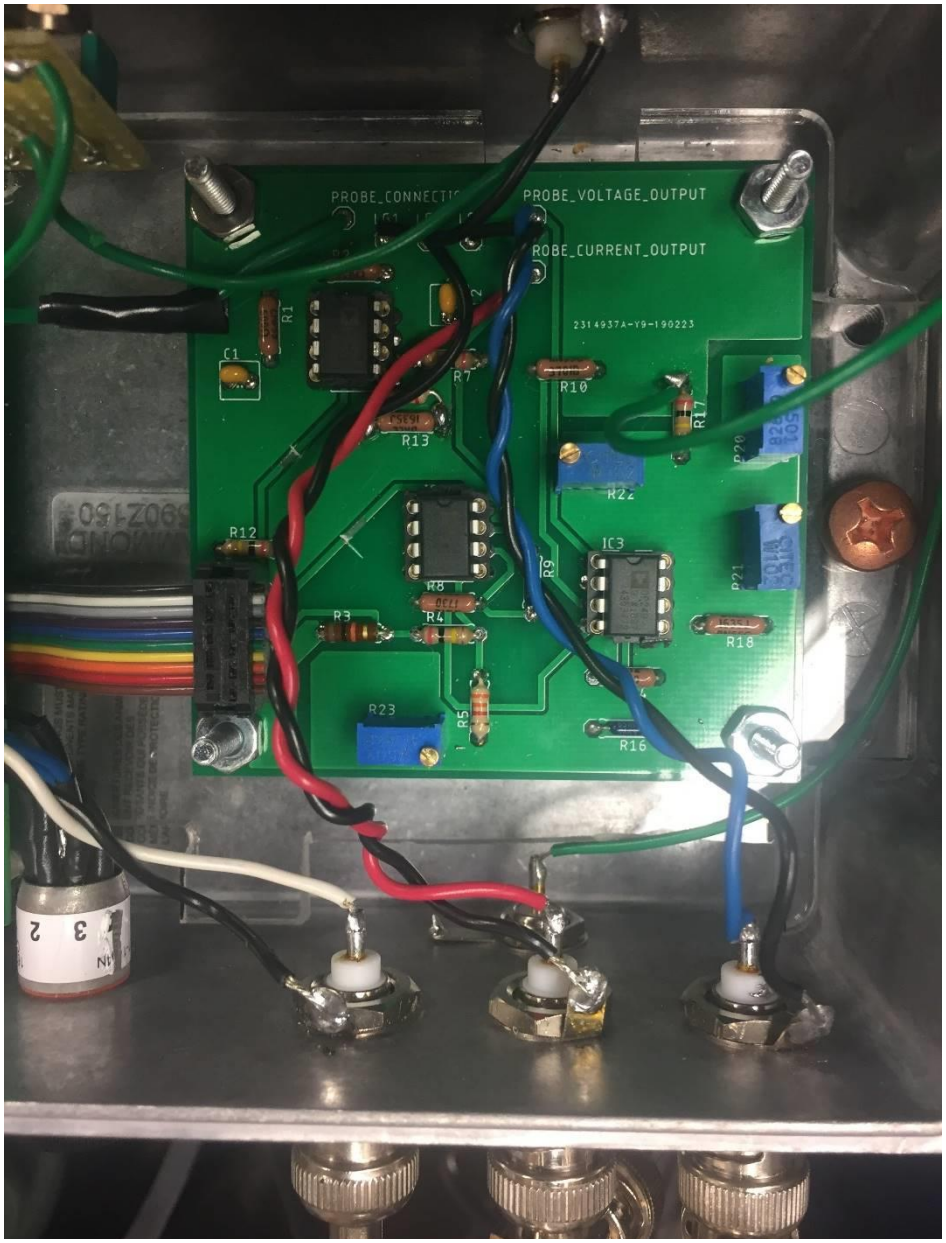

Figure 21 - Closer view of part 2 of 2 that make up the Langmuir probe sense circuitry.

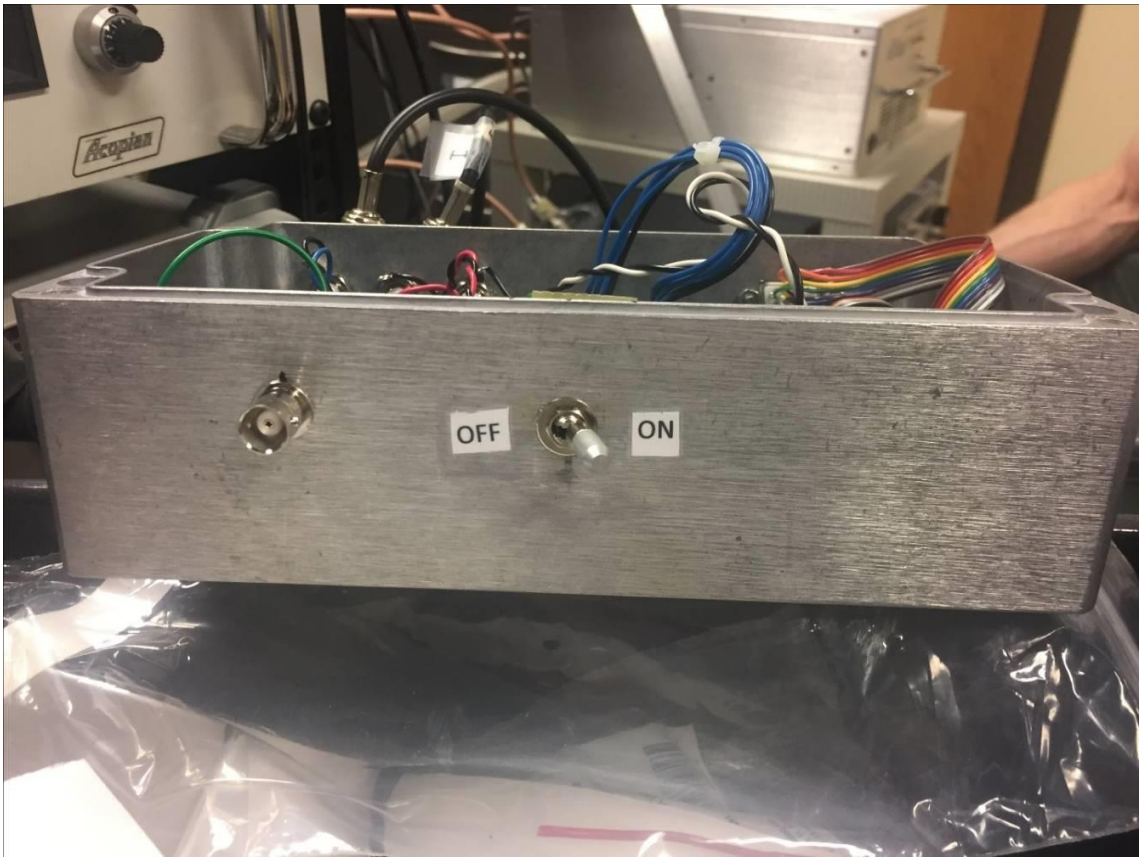

Figure 22 - Side view showing all inputs into the box, current sense range switch and, power input.

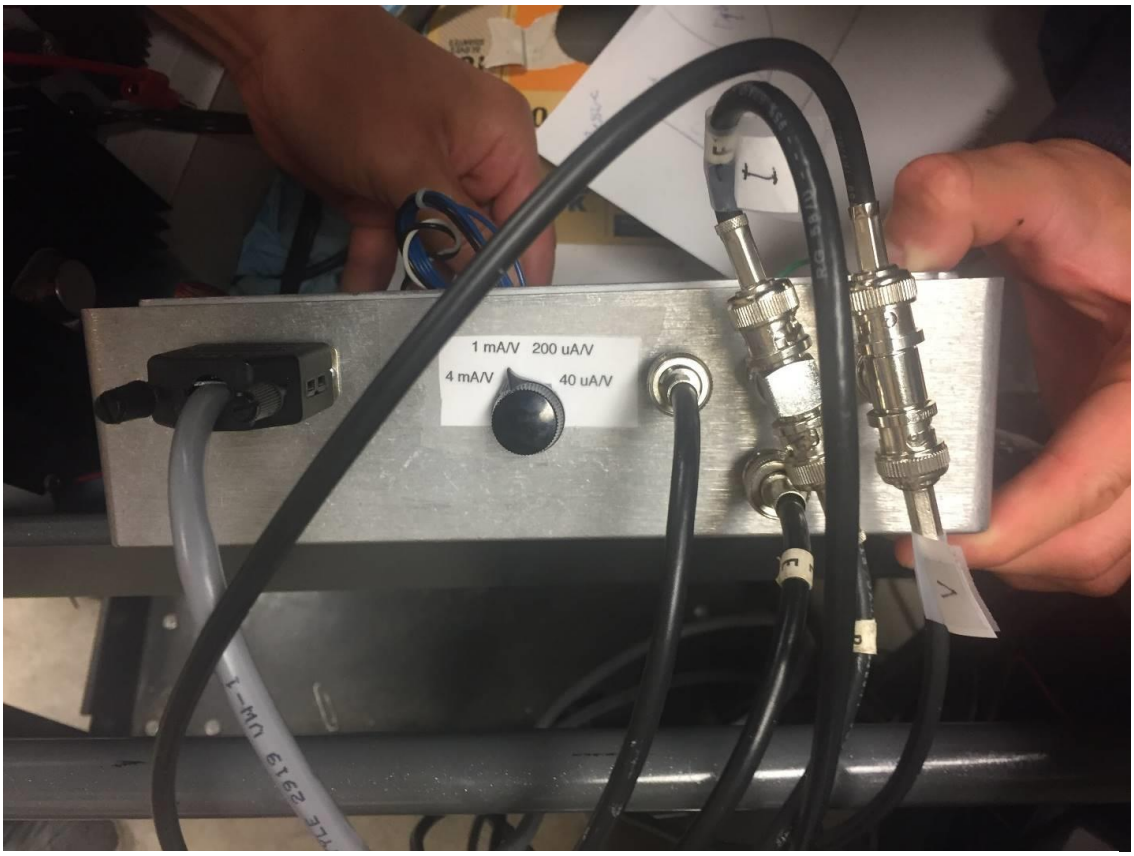

Figure 23 - Side view showing BNC connections to Langmuir probe and switch that connects and disconnects the probe form the circuit.

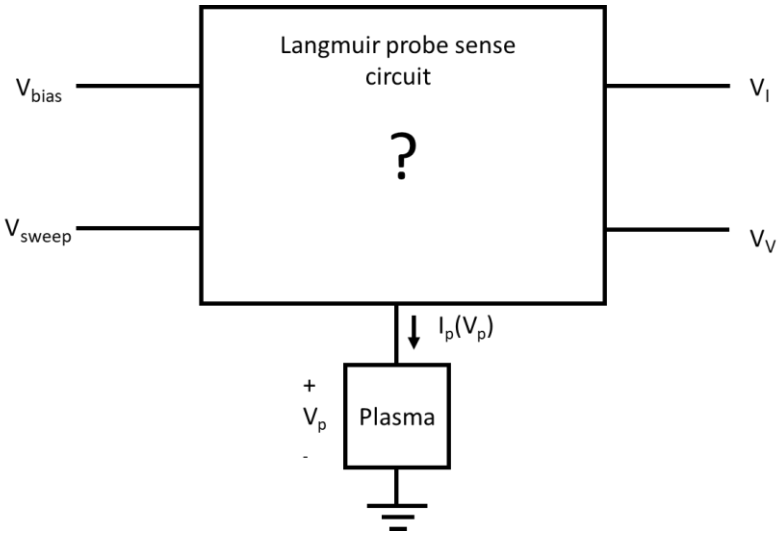

Figure 24 - Black box model of the Langmuir probe sense circuit.

What follows is an explanation on how the circuit is calibrated. The calibration of the circuit was accomplished on the assumption that the circuit behaved as a linear system in its operating range in which it is used in our experiments. Imagining the Langmuir probe sense circuit to be a black box as depicted in Figure 24, we have three inputs, namely V_{bias} (the DC bias set by the external voltage supply), V_{sweep} (the signal generated by a function generator), and I_p (the current flowing to and from the plasma); and two outputs which are the voltage signals V_V and V_I that correspond to the voltage and current at the probe tip. Assuming that the circuit has a linear relationship between its inputs and outputs then the most general set of equations that describe the circuit are the following:

$$V_I = aV_{bias} + bV_{sweep} + cI_p(V_p) + d \tag{4.1}$$

$$V_v = eV_{bias} + fV_{sweep} + gI_p(V_p) + h \tag{4.2}$$

$$V_p = jV_{bias} + kV_{sweep} + m \tag{4.3}$$

And by the nature of the circuit, $j = 1$ and so (4.3) is reduced down to

$$V_p = V_{bias} + kV_{sweep} + m \tag{4.5}$$

Further simplifying, if the circuit is properly adjusted then the previous three equations reduce down to the following:

$$V_I = cI_p(V_p) \tag{4.6}$$

$$V_v = V_{sw} \tag{4.7}$$

$$V_p = V_{bias} + V_{sweep} \tag{4.8}$$

So, by adjusting the circuit correctly the following constants would be,

$$a = b = d = e = g = h = m = 0$$

and,

$$f = j = k = 1$$

Ideally, calibration of the circuit would result in $(4.6) - (4.8)$ above. However, in the lab this mathematically exact adjustment is unobtainable. So, what can be done to calibrate the circuit as best as possible is to perform a calibration procedure that would let one solve for the constants in the equations above as well as solve for $I_p(V_p)$ when the outputs $V_V \; and \; V_I$ are known. Since V_{bias}, V_V, and V_I are known and if we have values for the constants in the above system of equations, then we could solve the system for the unknown parameters of interest, namely V_p, $I_p(V_p)$ and V_{sweep} since it too is not very well defined. So, this presents us with a system of three equations and three unknowns that we can solve using techniques of linear algebra.

The first step is to rewrite the equations in terms of the unknown parameters as follows:

$$V_I - aV_{bias} - cI_p(V_p) - d = bV_{sweep} \tag{4.9}$$

$$V_v - eV_{bias} - gI_p(V_p) - h = fV_{sweep} \tag{4.10}$$

$$V_p - V_{bias} - m = kV_{sweep} \tag{4.11}$$

We can eliminate V_{sweep} from the first two equations $(4.9) - (4.11)$ by solving both for V_{sweep} and setting them equal. A similar procedure can be done to set the second two equations equal to each other $(4.10) - (4.11)$ as well as for $(4.9)\ and\ (4.11)$. The combined equations are,

$$\frac{(V_I - aV_{bias} - cI_p(V_p) - d)}{b} = \frac{(V_v - eV_{bias} - gI_p(V_p) - h)}{f} \tag{4.12}$$

$$\frac{(V_V - eV_{bias} - gI_p(V_p) - h)}{f} = \frac{(V_p - V_{bias} - m)}{k} \tag{4.13}$$

$$\frac{(V_p - V_{bias} - m)}{k} = \frac{(V_I - eV_{bias} - cI_p(V_p) - d)}{b} \tag{4.14}$$

In eliminating V_{sweep} the only unknown parameters left to solve for are V_p and $I_p(V_p)$. (4.12) does not depend on V_p at all so we can solve it for $I_p(V_p)$ to get,

$$I_p = \frac{bV_V - fV_I + V_{bias}(fa - be) + fd - bh}{bg - fc} \tag{4.15}$$

and so (4.15) gives us $I_p(V_p)$ in terms of all the known parameters and the constants. We can then use (4.12) to solve for V_p from the expression above as follows,

$$V_p = V_{bias} + m + \frac{k}{f}\left(V_V - eV_{bias} - gI_p - h\right) \tag{4.16}$$

and so now (4.15) and (4.16) are the solutions to the linear portion of the system that arises from the circuit and the only thing left to find are the constants. These constants can be found by preforming the following tests on the circuit:

1) Set $V_{sweep} = I_p = 0$, vary V_{bias} and measure $\frac{\Delta V_I}{\Delta V_{bias}}$ and set the value equal to *a*.
2) Set $V_{bias} = I_p = 0$, vary V_{sweep} and measure $\frac{\Delta V_I}{\Delta V_{sweep}}$ and set the value equal to *b*.
3) Set $V_{bias} = V_{sweep} = 0$, inject known current into I_p measure $\frac{\Delta V_I}{\Delta I_p}$ and set it equal to *c*.
4) Set $V_{bias} = V_{sweep} = I_p = 0$, measure V_I and set the value equal to *d*.
5) Set $V_{sweep} = I_p = 0$, vary V_{bias} and measure $\frac{\Delta V_V}{\Delta V_{bias}}$ and set the value equal to *e*.
6) Set $V_{bias} = I_p = 0$, vary V_{sweep} and measure $\frac{\Delta V_V}{\Delta V_{sweep}}$ and set the value equal to *f*.
7) Set $V_{bias} = V_{sweep} = 0$, inject known current into I_p and measure $\frac{\Delta V_V}{\Delta I_p}$ and set it equal to *g*.
8) Set $V_{bias} = V_{sweep} = I_p = 0$, measure V_V and set the value equal to *h*.
9) Using a voltmeter, vary V_{sweep}, measure V_p, calculate $\frac{\Delta V_p}{\Delta V_{sweep}}$ and set it equal to *k*.

10) Using a voltmeter, set $V_{bias} = V_{sweep} = 0$, measure V_p and set it equal to *m*.

With the above constants measured (4.15) and (4.16) can then be used along with the known V_{bias}, V_V, and V_I data to generate an I-V characteristic plot of the RF plasma in our experiments. The above calibration procedure was thought up and implemented by Dr. Karl Stephan.

V. EXPERIMENTAL PROCEDURE AND RESULTS

The previous section focused on the design and construction of the Langmuir probe sense circuitry. In this section, we discuss the function of the circuit in the system as shown in Figure 25. From the previous section we see that the probe circuit is connected to a DC bias supply and an arbitrary waveform generator. The DC bias supply is connected to the floating ground potential and so, whatever value the supply is set to, the floating ground follows suit with respect to the system ground potential. As a result, the probe tip is raised or lowered to the respective DC bias potential. On the other hand, the waveform generator is then set up to generate a triangle wave of specific frequency and amplitude. This signal is connected to the non-inverting portion of an operational amplifier whose output follows the signal and is connected to a push-pull configuration of transistors that supply the current to the Langmuir probe tip.

The current that is sourced and sunk by the probe is measured by the AMPO1EX instrumentation amplifier whose input terminals are connected across the current sensing resistors in the circuit schematic shown in Figure 15 in the section about the construction of the probe. The voltage drop across the sensing resistors is then sent to a voltage level shifter whose job it is to subtract off the DC bias supply from the measured signal to give the actual voltage drop relative to the system ground across the resistor that can then be used to calculate the current into or out of the probe.

On the probe side of the current sense resistors there is a follower amplifier stage that is used as a voltage buffer to measure the voltage at the probe tip relative to the floating ground. The voltage signal from the buffer is then connected to another voltage

level shifting stage that, just as the last voltage level shifting stage mentioned, subtracts off the DC bias the probe tip is raised to.

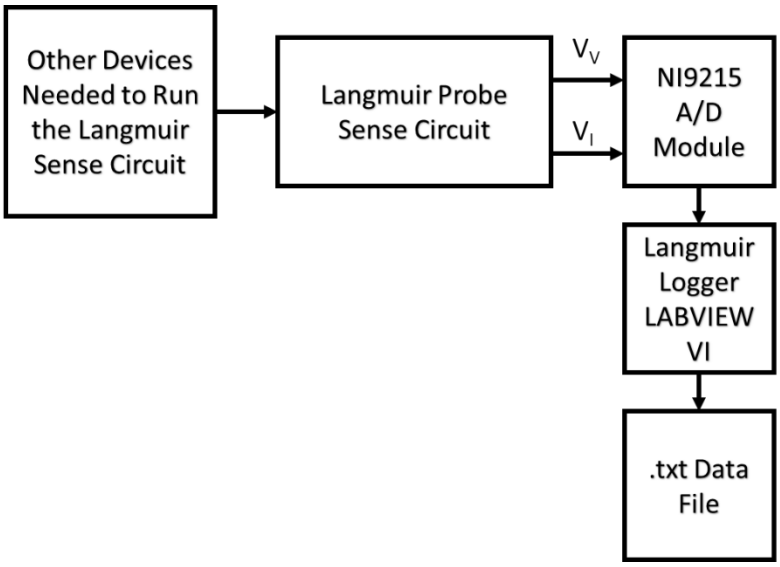

Figure 25 - Functional block diagram of how a data file is made with the Langmuir sense circuit and the logger IV.

The two voltage outputs of the level shifting stages are then sent out to an NI9215 A/D converter box that has a LABVIEW VI written by Dr. Karl Stephan that processes the data and stores it in a .txt file. The VI sorts the incoming voltage values from least to greatest and pairs the voltage values with their corresponding current values. The data is then stored in two column vectors in a .txt file as stated previously.

Figure 26 below is a screen shot of the graphical user interface for the Langmuir Logger used to collect data from the Langmuir probe sense circuit. Starting from the top left, in the portion of the Logger that is labeled Before Logging:, there are 5 boxes below the label. The first box is used to designate a file path to save the data to, the second is used to choose a filename for the data collected and the next three boxes are used to insert comments over the measurement conditions.

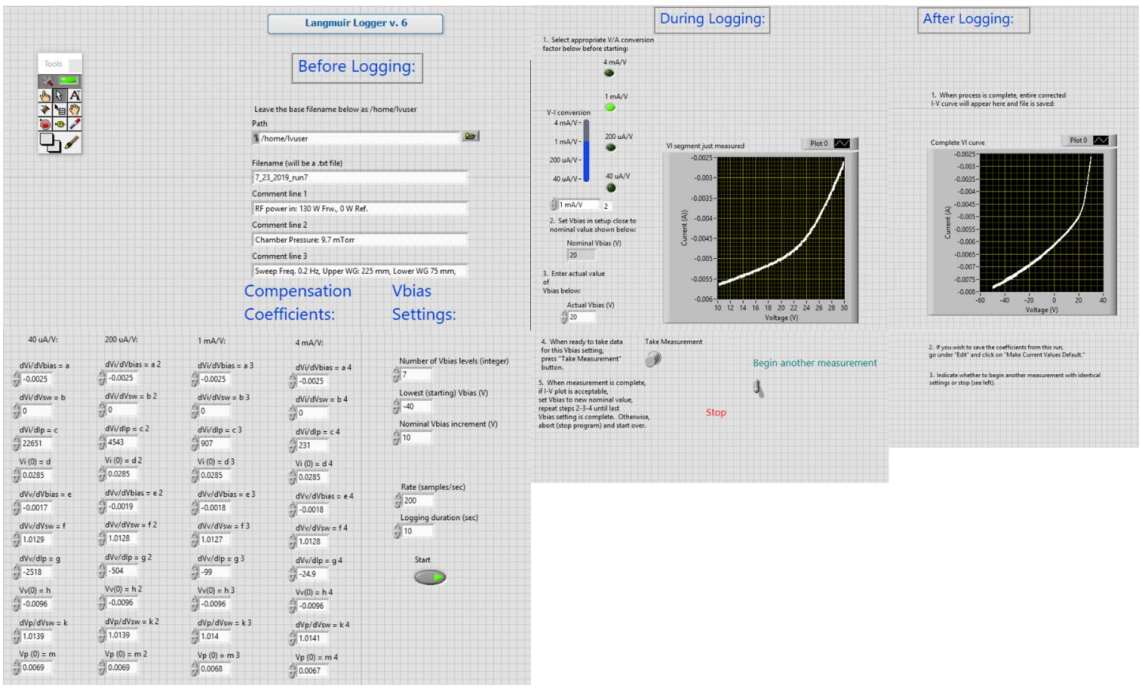

Figure 26 - Graphical user interface for collecting I-V data from Langmuir probe sense circuit.

Below the comment boxes, in the space labeled Compensation Coefficients: is where according to the instructions mentioned on the last section, the measured coefficients for each sense resistor range can be input into the program. The IV takes these coefficients and uses them to calculate the corrected probe voltage and current as described in the last section for a given current sensing range. Moving over to the right under the label that says Vbias Settings:, the first box labeled Number of Vbias levels (integer) requires the user to input an integer number for the number of DC bias levels where measurements will be taken. Below the number of Vbias levels is the Lowest (starting) Vbias (V) box, where the user enters the lowest DC bias that will be used for a run. Next, Nominal Vbias increment (V), box is where the increment of Vbias steps is input. The last two boxes below Nominal Vbias increment (V) are for inputting a sample rate and a logging duration time. With all of those parameters set the virtual button

labeled Start is pressed after the run button at the top of the LABVIEW VI window is pressed and the program is ready to run its first measurement.

In the next window labeled During Logging the current sense range is selected and made to match the knob on the Langmuir sense circuit box. The DC bias that the user needs to set the DC supply into the Langmuir probe sense circuit is labeled Nominal Vbias (V). Below this prompting box is Actual Vbias (V) where the user inputs the approximate value the DC bias is set to so that the corresponding data taken for that specific DC bias can be centered around its respective DC bias. After the actual Vbias is set, the measurement can be taken by pressing the button labeled Take Measurement. The measurement lasts the logging duration and then the collected data is displayed on the IV plot labeled VI segment just measured. Once all of the measurements have been taken the segments are pieced together and plotted in the graph pictured below the label After Logging: named complete VI curve.

For calculations of electron density n_e, which is the parameter of most interest for this study, orbital-motion-limited (OML) theory was used. According to Chen [10] if we assume that plasma conditions are set so that the plasma sheath edge (distance between the Langmuir probe and the furthest reaching portion of the plasma sheath) is much greater than the radius of the probe then an application of OML theory is justified. In the limit as the ion temperature approaches zero then the ion saturation current can be approximated by,

$$I_i(V_p) \approx \frac{A_p n_e e\sqrt{2}}{\pi}\sqrt{\frac{|eV_p|}{m_i}} \tag{5.1}$$

In (5.1) above, V_p is the effective probe potential and can be written as the difference between a constant related to the plasma potential V_s and the potential of the probe V_{pr}. So, V_p can be written as,

$$V_p = V_s - V_{pr} \tag{5.2}$$

If we only consider $V_p > 0$ then (5.1) can be simplified down to the following equation with two undetermined constants namely A and B. The equation is given by,

$$I(V_{pr}) = A(B - V_{pr})^{\frac{1}{2}} \tag{5.3}$$

where $A = \frac{A_p n_e e\sqrt{2}}{\pi}\sqrt{\frac{e}{m_i}}$ and $B = V_s$. With a sufficiently negative bias applied to the Langmuir probe (V_{pr} < -20V) it is safe to assume that the electron current to the Langmuir probe is so small that it is negligible, and the equations derived from OML theory above are valid. So the first step in the analysis to determine n_e is to use two voltages at or below -20V and their corresponding currents to calculate a numerical value for *B*. An expression for *B* can be found by taking a ratio of (5.3) for the two different voltage and current values as depicted below,

$$\frac{I_1}{I_2} = \frac{A(B - V_1)^{\frac{1}{2}}}{A(B - V_2)^{\frac{1}{2}}} \tag{5.4}$$

Solving (5.4) for *B* gives,

$$B = \frac{V_2\left(\frac{I_1}{I_2}\right)^2 - V_1}{\left(\frac{I_1}{I_2}\right)^2 - 1} \tag{5.5}$$

And so using the two voltages chosen that satisfy the criteria above will give *B* which in turn can be used to solve for *A* and thus n_e. Rewriting (5.3) above for *A* gives,

$$A = \frac{I_1(V_1)}{(B - V_1)^{\frac{1}{2}}} \tag{5.6}$$

Finally, solving A for n_e from the definition of *A* we get,

$$n_e = \frac{A\pi}{A_p e}\sqrt{\frac{m_i}{2e}} \tag{5.7}$$

So, as a sample calculation, in our experimental setup the diameter of the probe tip is 304.8 μm and the length of the probe that extends into the plasma is 1.06 cm. If only the surface area of the probe exposed to the plasma along the probes axis is taken into account and not the probe tip then A_p of the probe is given by,

$$A_p = 2\pi\left(\frac{d}{2}\right)l = 2\pi\frac{304.8 * 10^{-6}\, m}{2}(0.0106\, m) = 1.015 * 10^{-5} m^2 \tag{5.8}$$

The mass of an argon (the working gas in the system used) atom in kilograms is,

$$m_{iAr} = \left(1.6605 * \frac{10^{-27} kg}{amu}\right)(39.948 amu) = 6.633 * 10^{-26} kg \tag{5.9}$$

and now simplifying the constants found in (5.7) we get,

$$n_e = (A * 8.790 * 10^{20}) m^{-3} \tag{5.10}$$

So, we can now write n_e as a function of a sufficiently negative voltage and corresponding current point from the data collected as,

$$n_e = \left(\frac{I_1(V_1)}{(B - V_1)^{\frac{1}{2}}} 8.790 * 10^{20} \right) cm^{-3} \tag{5.11}$$

Without derivation the following equation can be used to calculate the electron temperature for the data collected:

$$T_e(V_e) = \frac{V_2 - V_1}{\ln\left(\frac{I_2}{I_1}\right)} \tag{5.12}$$

However, (5.12) is said to give only rough approximations to the electron temperature values for the data collected from our system, perhaps because we are unable to find the electron saturation region using our probe and driver circuit before it begins to exhibit breakdown behavior.

An Excel spreadsheet was prepared to calculate a running average of 20 data points either side of the data point being considered to smooth the data set. The user of the spreadsheet then chooses a sufficiently negative pair of voltage points and their corresponding currents to calculate values for *A* and *B* in the equations above. A model curve is then fit to the data set using (5.3) above and the user can decide if the curve is a good fit. If the curve fits well then, a data point is selected from the portion of the raw data set that also seems to fit the model well and is then used in (5.11) aabove to calculate the value of n_e. From the same best fit curve plot, two voltage entries and their corresponding currents can be chosen to use in (5.12) to finds the electron temperature, in principle.

The method described above for finding n_e and T_e was used to process I-V data collected from an OA4G cold-cathode gas-filled vacuum tube and data collected on the RF plasma chamber built. A 20-point running average curve for the OA4G vacuum tube is depicted in Figure 27. Roughly the dimensions of the probe tip inside of the OA4G vacuum tube are 7.6 ± 0.2 mm for its diameter and 25.4 ± 0.2 mm for its length and the gas within the tube is argon. [9] The effective surface area that is used for the calculation of n_e above is $0.6064 * 10^{-3} \pm 0.0002\ m^2$. The DC plasma formed within the OA4G vacuum tube had the following electrical bias characteristics: potential at the anode was $V_{anode} = 73.1V$ and the current flowing through the anode $I_{anode} = 7mA$. The data was then processed using the Excel spreadsheet mentioned above.

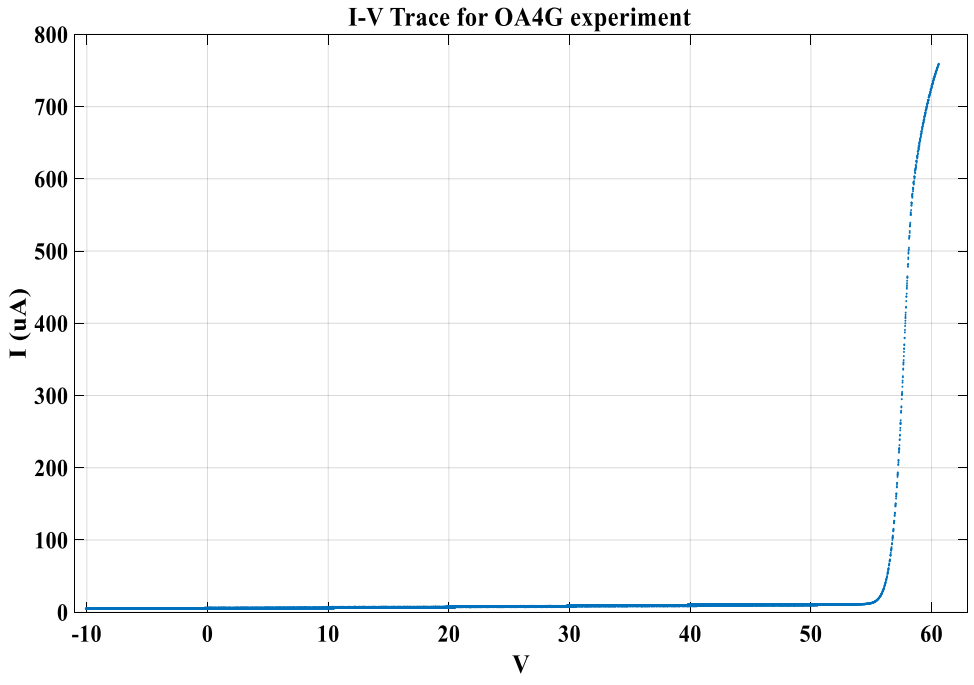

Figure 27 - Typical IV trace of an OA4G vacuum tube used as a plasma chamber.

Table 1 - Voltage and current values used to calculate n_e.

Data Point	Voltage	(-1)*Current (μA)
1	-9.984	4.9905
2	-9.012	4.935

Then a data point (V,I) within the voltage range $[V_1, V_2]$ is selected to calculate n_e, which in this case was (-9.582, 5.04605) and the electron density was calculated to be $1.125 * 10^{14}\ cm^{-3}$. In comparison to the results gathered in [9] the electron density value calculated using OML theory differs by about two orders of magnitude more than what Williams found for the same device (OA4G vacuum tube). The values used to calculate the electron temperature are given in the following table:

Table 2 - Voltage and current values used to calculate T_e.

Data Point	Voltage	Current (μA)
1	56.652	86.7384
2	57.965	457.3523

Using the voltage and current values in Table 2 the electron temperature value was found to be approximately 1.818 eV which is about 1.4 more electron volts then what Williams reported. Differences in electron density may have arisen due to not using the same theories to calculate n_e and T_e.

The experiment and data analysis conducted on the OA4G vacuum tube was performed as a check on how well the Langmuir probe system was working. By comparing the values of n_e and T_e that we derived from the data to that of what was presented in [9] we can have some reassurance that the probe is functioning the way that it should. After verifying that the driver circuit was working properly, the circuit was connected to the custom RF plasma chamber with the Langmuir probe mentioned in a previous section. Figure 28 shows a sample I-V trace gathered by the custom-built Langmuir probe and driver circuit and associated data collection hardware and software. Using the same analysis as outlined above we can derive n_e and T_e values from the data

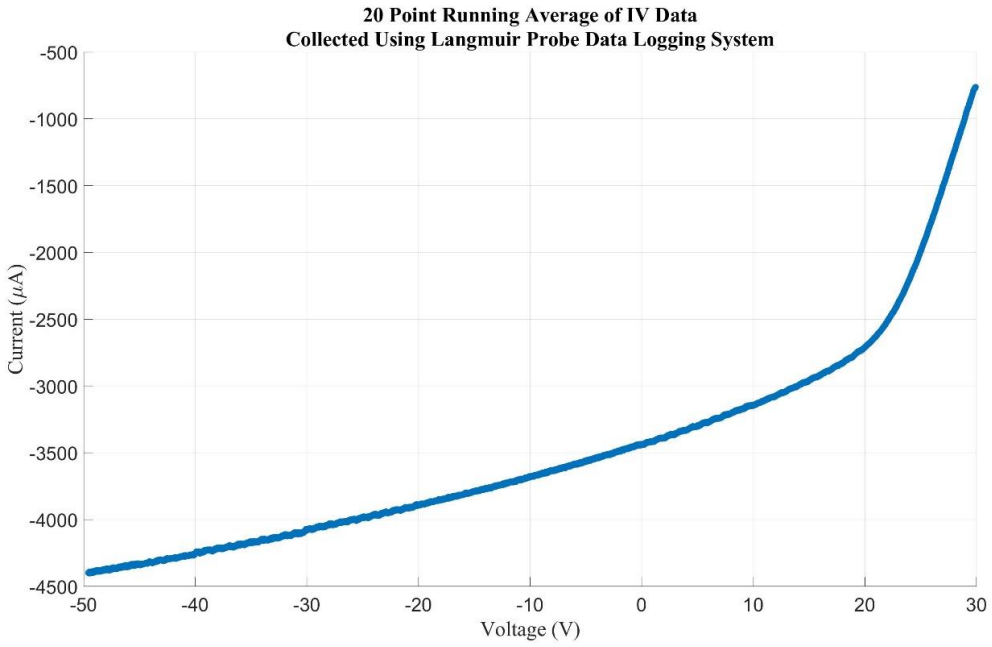

Figure 28 - Running average data set taken from a 50 W RF plasma in custom made RF plasma chamber.

set collected from the RF plasma chamber.

Referring to Table 3, the voltage and inverted current values were used to calculate the value of $n_e = 3.48 * 10^{11} cm^{-3}$ and the value that follow in Table 4 are those used to find the value of $T_e = 29.24\ eV$.

Table 3 - Voltage and current values used to calculate n_e for a 50 W, approximately 9 mTorr RF plasma.

Data Point	Voltage	(-1)*Current (μA)
1	-30.032	4079.97
2	-10.003	3678.50

Table 4 - Voltage and current values used to calculate T_e for a 50 W, approximately 9 mTorr RF plasma.

Data Point	Voltage	(-1)*Current (μA)
1	2.26	97
2	7.19	143

The derived electron density value seems like a reasonable value for a laboratory RF plasma if we compare our value to that obtained in the literature using similar setups (referring to RF power input and chamber pressures used) then the parameter is reasonable.

VI. CONCLUSION

In trying to figure out a relationship between how the electron density of a cylindrically symmetric RF plasma affects the transmission of microwave radiation transmitted between waveguides we needed a way to measure the electron density. Obviously, a commercial Langmuir probe could be used to find the parameters of interest to our experiments. However, the cost of a commercial Langmuir probe was simply not within the budget of the principal investigator prior to the time of this writing. The only option available to us was to build a custom Langmuir probe and the associate probe driver circuit.

The literature on Langmuir probes and the theory explaining how they work is quite extensive so there was no problem in finding a suitable design and driver circuit that would work for us. However, in our search for a solution we did run into problems with driver circuit designs. The first attempt at a Langmuir probe driver circuit led us to face issues with improper grounding, too small of a voltage range for which we can drive the circuit, and noise interfering with our measurements. Luckily, we did not have to try more than two circuit designs till we found one that worked for our experiments. The Langmuir probe driver circuit taken from [9] eliminated problems arising from not properly isolating the two ground planes used for making the measurement, as well as allowing a larger voltage range for the IV sweep. The noise issues that came with the earlier versions of the driver circuit were overcome by building and tuning the RF chokes with high enough Q and for the right frequency to be attenuated coming into the driver circuit. Use of an isolation transformer from mains voltage to the main linear voltage regulating power supply also helped to eliminate further noise issues.

With the driver circuit and the probe functioning, data collection was possible, but we failed to collect an IV curve that captured the custom-built RF plasma chamber's electron saturation region. From the electron saturation region, we initially intended to derive electron density values, but a common trend among the data curves we collected was that unless the voltage was dropped below a certain point where our probe seemed to exhibit some type of breakdown phenomenon, we obtained a reasonably good-looking exponential increasing current region but no electron saturation region. At a sufficiently positive potential, instead of the expected electron saturation region, again a similar breakdown phenomenon occurred to when the potential was sufficiently negative.

Since the electron saturation region did not seem to be obtainable from our plasma system we chose to see if OML theory could be applied to our setup. With the proper assumptions we could fit our data set to OML theory model and then use the model to derive values for the electron density and temperature of our RF plasma. With regard to future work, we still need to analyze more data sets taken on different days and compare the electrical plasma parameters of interest to one another. In doing so we will be able to see if our measurement system is consistent. Also, it should be possible to write a MATLAB program that will allow easy data analysis as well as plotting so that we can get the analysis done faster than by using the Excel spreadsheet.

LITERATURE CITED

[1] H. -C. Wu, "Relativistic-microwave theory of ball lightning," Nature SCIENTIFIC REPORTS, vol. 6, no. 28263, pp. 1-8, 2016. Type first entry using style approved by committee.

[2] I. H. Hutchnison, "Plasma Particle Flux," in Principles of Plasma Diagnostics, Massachusetts, Cambridge University Press, 2005 , 2005, pp. 55-72.

[3] A. Piel, "Plasma Boundaries," in Plasma Physics An Introduction to Laboratory, Space, and Fusion Plasma, Cham, Switzerland, Springer, 2017, pp. 175-209.

[4] A. P. Paranjpe, J. P. McVittie and S. A. Self, "A tuned Langmuir probe for measurments in RF Glow discharges," AIP J. Appl. Phys., vol. 67, no. 11, pp. 6718-6727, 1990.

[5] F. F. Chen, "Langmuir probes in RF plasma: surpring validity of OML theory," IOP Plasma Sources Science and Technology, no. 18, p. 13, 29 May 2009.

[6] F. F. Chen, "Time-Varying impedance of the sheath on a probe in an RF plasma," IOP Plasma Sources Science and Technology, vol. 15, pp. 773-782, 2006.

[7] I. D. Sudit and F. F. Chen, "RF compensated probes for high-density discharges," IOP Plasma Sources Science and Technology, vol. 3, pp. 162-168, 1994.

[8] R. L. Merlino, "Understanding Langmuir probe current-voltage characteristics," Am. J. Phys. American Assosciation of Physics Teachers, vol. 75, no. 12, pp. 1078-1085, 2007.

[9] J. Williams, "WUPL," 27 July 2014. [Online]. Available: http://wupl.wittenberg.edu/curricular/AAPT2014.html. [Accessed 1 January 2019].

[10] F. F. Chen, "Lectrue notes on Langmuir probe diagnostics," Los Angeles, 2003.